European Journal of Medicinal Chemistry 297 (2025) 117964

Contents lists available at ScienceDirect

European Journal of Medicinal Chemistry

journal homepage: www.elsevier.com/locate/ejmech

Research paper

Hunting for lubeluzole analogues as antimyotonic agents with reduced cardiac liability

Maria Maddalena Cavalluzzi [a,*], Roberta Gualdani [b], Alessandro Farinato [a], Concetta Altamura [c], Sabata Pierno [a], Natalie Paola Rotondo [a], Francesco Terlizzi [a], Laura Beatrice Mattioli [d,e], Maria Grazia Perrone [a], Maria Cristina Lomuscio [f], Giuseppe Felice Mangiatordi [g], Nicola Antonio Colabufo [a], Antonio Carrieri [a], Roberta Budriesi [d], Peter Gmeiner [h], Harald Huebner [h], Jean-François Desaphy [c], Giovanni Lentini [a]

[a] Department of Pharmacy–Pharmaceutical Sciences, University of Bari Aldo Moro, 70125 Bari, Italy
[b] Institute of Neuroscience, Université Catholique de Louvain, Brussels, Belgium
[c] Section of Pharmacology, Department of Precision and Regenerative Medicine, School of Medicine, University of Bari Aldo Moro, 70124 Bari, Italy
[d] Department of Pharmacy and Biotechnology, Food Chemistry and Nutraceutical Lab, Alma Mater Studiorum-University of Bologna, 40126 Bologna, Italy
[e] Health Sciences and Technologies-Interdepartmental Center for Industrial Research (CIRI-SDV), Alma Mater Studiorum University of Bologna, Bologna, Italy
[f] Department of Precision and Regenerative Medicine and Jonian Area, University of Bari Aldo Moro, Piazza Giulio Cesare, 11, Policlinico, 70124, Bari, Italy
[g] CNR – Institute of Crystallography, 70126 Bari, Italy
[h] Department of Chemistry and Pharmacy, Friedrich-Alexander University, 91058 Erlangen, Germany

ARTICLE INFO

Keywords:
Lubeluzole
hERG liability
Sodium-channel blockers
Use-dependence
Myotonia

ABSTRACT

Lubeluzole is a neuroprotective agent displaying antimyotonic activity. Lubeluzole clinical development as an antiischemic drug was discontinued due to a lack of efficacy in human trials and possible cardiac toxicity. Since lubeluzole is a potent inhibitor of the hERG channel, involved in long QT syndromes and the potentially fatal cardiac arrhythmia Torsade de Pointes, a series of lubeluzole analogues were prepared to investigate the structural requirements to reduce the affinity for hERG channels to possibly obtain safe antimyotonic drugs. Compound **16o** was identified as the less potent hERG blocker possibly endowed with lower cardiac liability in comparison with the parent compound. Antimyotonic activity of **16o** was also investigated in vitro on hNav1.4 and higher use-dependence was observed in comparison to lubeluzole, thus suggesting greater selectivity toward highly excited tissues, such as the myotonic muscle. To further verify the cardiac safety of **16o**, patch-clamp experiments on hNav1.5 were also carried out and a 3-fold reduction of potency in comparison with hNav1.4 in phasic block was observed. In vivo evaluation of the antimyotonic activity showed unintended effects on rat motor performance. Ex vivo studies suggested calcium channel blocking activity as a possible off-target source of the **16o** unintended effects, also reinforced by possible interaction with β_2 receptors, as indicated by in vitro binding assays and in silico studies. In conclusion, we think our results may support the rational design of lubeluzole analogues endowed with both antimyotonic activity and lower hERG liability.

1. Introduction

Lubeluzole (Fig. 1) is a neuroprotective agent originally investigated for its potential benefits in the treatment of ischemic stroke but whose clinical trials were discontinued due to a lack of benefits in humans in terms of survival after ischemic injury [1,2]. Moreover, a significant increase in heart conduction disorders was also observed in the treated patients [2,3], suggesting a possible association of lubeluzole with acquired long QT syndrome and ventricular arrhythmias [4]. In an attempt to repurpose lubeluzole in new therapeutic applications, our efforts have been devoted in the last two decades to identifying new biological activities at concentrations lower than those responsible for its cardiac liability, including chemosensitizing [5,6] and antidiarrheal effects [7]. In addition, we demonstrated that lubeluzole is a potent inhibitor of the human skeletal muscle voltage-gated sodium channels hNav1.4 and displays a potent antimyotonic activity in an animal model

* Corresponding author.
E-mail address: mariamaddalena.cavalluzzi@uniba.it (M.M. Cavalluzzi).

https://doi.org/10.1016/j.ejmech.2025.117964
Received 6 May 2025; Received in revised form 7 July 2025; Accepted 8 July 2025
Available online 10 July 2025

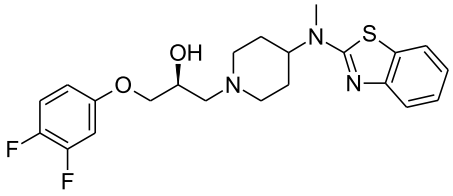

Fig. 1. Lubeluzole structure.

of Myotonia Congenita, a rare disease characterized by skeletal muscle hyper-excitability and stiffness [8,9]. These results prompted us to include lubeluzole in a list of sodium channel blocker candidates for repositioning [10]. Given the severity of the side effects observed during the clinical trials, we finally explained the lubeluzole-induced QT interval prolongation as possibly related to the inhibition of the human ether-a-go-go-related gene (hERG) channel, which may preclude further human use [4]. Herein, we aimed at understanding the molecular determinants of hERG channel inhibition through a series of lubeluzole congeners prepared in their racemic form, having previously observed the lack of stereoselectivity of lubeluzole interaction with both hERG and Nav1.4 channels [4,8]. Searching for novel and safer antimyotonic agents, the Nav1.4 sodium channel-blocking activities of the most promising compound – the dihydroxylated analogue **16o** – have also been evaluated for its in vivo activity in a rat model of myotonia.

2. Results and discussion

2.1. Chemistry

All the target compounds [(*RS*)-**8,** (*RS*)-**15f–m,** and (*RS*)-**16n,o**] were prepared through convergent syntheses, as depicted in Schemes 1 and 2. The first synthesized analogue [(*RS*)-**8**] was obtained according to the literature procedure previously reported for lubeluzole [11], with minor modifications (Scheme 1). *N*-Methyl-*N*-piperidin-4-yl-1,3-benzothiazol-2-amine (**5**) was obtained starting from ethyl 4-oxopiperidine-1-carboxylate (**1**) which was submitted to direct reductive amination with methylamine hydrochloride to give the intermediate **2** which was converted into the corresponding *N*-benzothiazole derivative **4**, in turn deprotected in 48% hydrobromic acid to give the benzothiazole-2-amine **5**. In parallel, (*RS*)-2-(phenoxymethyl)oxirane [(*RS*)-**7**] was obtained through the Williamson procedure, using greener reaction conditions [12] than those previously adopted in our laboratory for the synthesis of aryl alkyl ethers [11,13,14]. The so-obtained oxirane intermediate (*RS*)-**7** was submitted to $Yb(OTf)_3$-catalyzed aminolysis with **5** to provide (*RS*)-**8**.

Compounds **15f**–**m** and **16n,o** were prepared according to the more concise synthetic route described in Scheme 2, avoiding the *N*-ethoxycarbonyl deprotection step carried out in Scheme 1. The oxirane intermediates (*RS*)-**10a,b** reacted under microwave irradiation with piperidine-4-one, previously extracted from its commercially available hydrochloride salt, and the so-obtained intermediates (*RS*)-**11a,b** were submitted to reductive amination in a microwave reactor [15,16] to give the secondary amines (*RS*)-**12a,b**. Variously substituted 2-chlorobenzothiazoles (**14c–e**, with **14e** having been obtained starting from **14c**), in turn obtained submitting the corresponding amines **13c,d** to the Sandmeyer reaction with copper(II) chloride and *tert*-butyl nitrite [17], were reacted with (*RS*)-**12a,b** to give the compounds (*RS*)-**15f–m**. Finally, deprotection of (*RS*)-**15l,m** with $AlCl_3$ gave the analogues (*RS*)-**16n,o**.

2.2. In-silico pharmacokinetics and hERG-related cardiotoxicity evaluation

All the synthesized compounds underwent in-silico profiling of relevant pharmacokinetic properties and their potential as hERG blockers (Table 1). For this purpose, we utilized the QikProp tool,

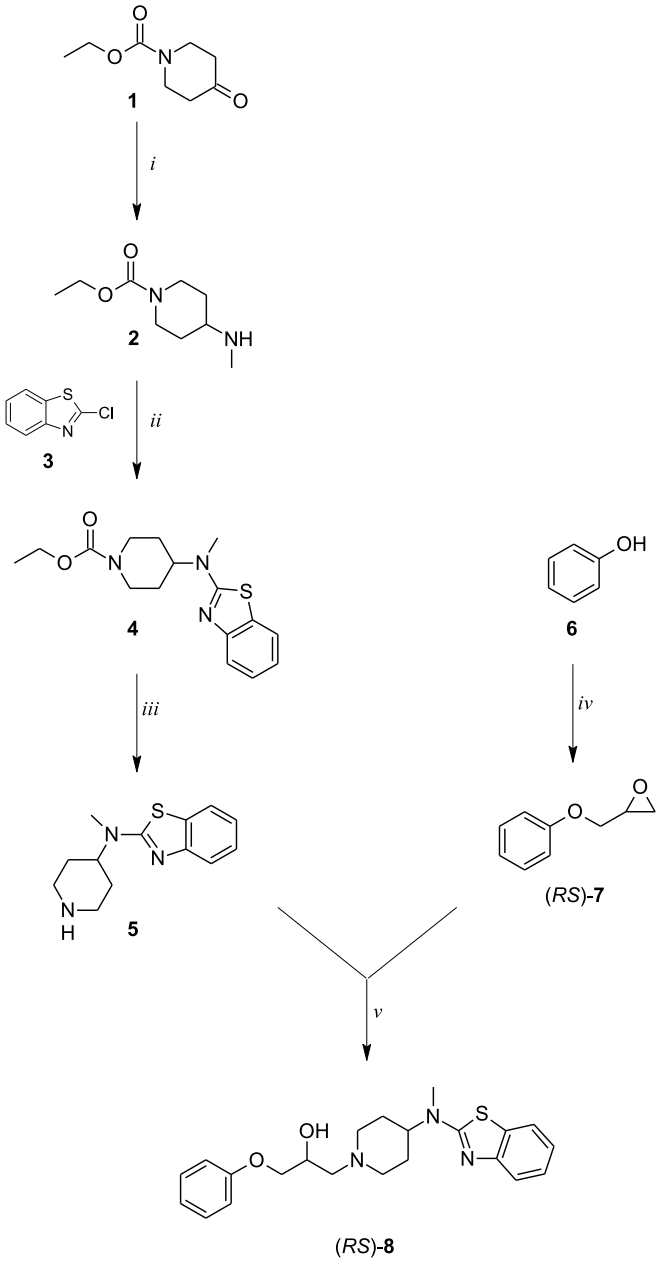

Scheme 1. *Reagents and conditions:* (i) methylamine hydrochloride, $NaBH_3CN$, MeOH; (ii) 2-chloro-1,3-benzothiazole, TEA, $(CH_2OH)_2$; (iii) 48% HBr; (iv) (*RS*)-epichlorohydrin, NaOH, H_2O, reflux, 3 h; (v) $Yb(OTf)_3$, anhyd. CH_2Cl_2.

available from the Schrödinger suite 2022-4 [18]. Initially, our focus was on the QPlogPo/w parameter, which predicts the octanol/water partition coefficient. Increased lipophilicity is known to enhance a molecule's likelihood of binding to hERG [19–21]. Specifically, we assessed the lipophilicity drop resulting from the replacement of fluorine atoms on the aryloxy moiety with more polar substituents (**15l,m** and **16n,o**), observing that compound **16o** returned the lowest value (2.02), while **15h**, featuring the CF_3 group on the 6-benzothiazole position, exhibited the highest QPlogPo/w value (4.59). It is recognized that an ideal antimyotonic candidate should not penetrate the blood-brain barrier to avoid undesired effects in the central nervous system (CNS). Furthermore, oral administration is highly desirable for user-friendly chronic treatment. With this in mind, we computed descriptors related to CNS activity and oral absorption in humans, including: (i) CNS, providing an estimation of CNS activity on a scale from −2 (inactive) to

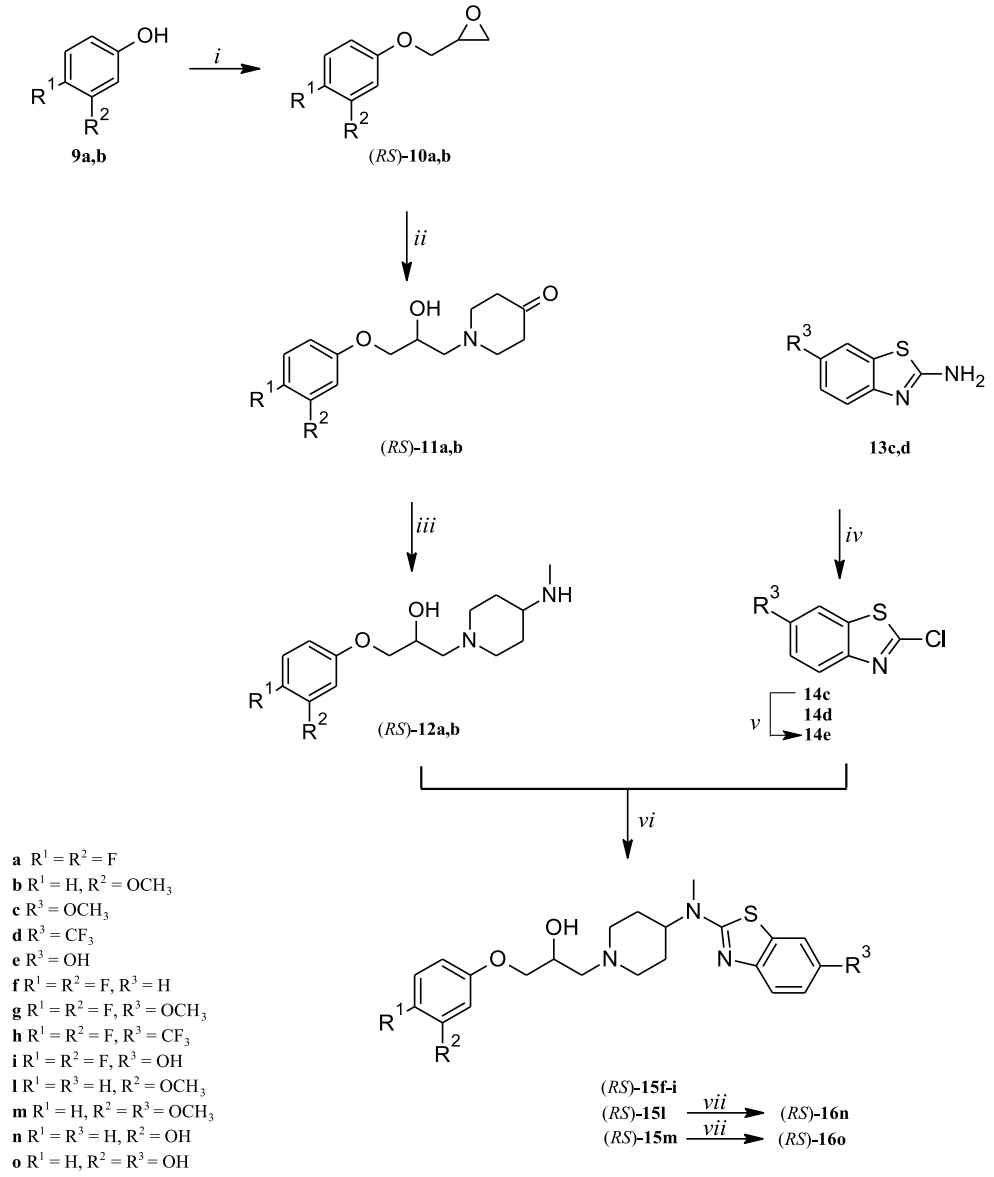

Scheme 2. *Reagent and conditions:* (i) (*RS*)-epichlorohydrin, Cs_2CO_3, acetonitrile, reflux, 17 h; (ii) MW, piperidine-4-one, CH_2Cl_2, 100 °C, 8–12 min; (iii) MW, methylamine hydrochloride, $NaBH_3CN$, MeOH, 110 °C, 11 min; (iv) *tert*-butyl nitrite, $CuCl_2$, acetonitrile, room temp, 2 h, then 70 °C, 1 h (reflux, 30 min for **13d**); (v) $AlCl_3$, toluene, 110 °C, 1 h; (vi) TEA ($NaHCO_3$ for **15l**), H_2O, 110 °C, 10 h; commercially available 2-chlorobenzothiazole for **15f**; (vii) $AlCl_3$, toluene, 110 °C, 18 h.

Table 1
Some pharmacokinetic and pharmacodynamic properties computed for the compounds under investigation. Notice that the tool QikProp, available from the Schrodinger suite 2022-4, was employed to compute all the properties.

	QPlogPo/w	QPIC$_{50}$HERG (nM)	CNS	QPlogBB	QPPMDCK	QPPCaco	PercentHuman OralAbsorption
Lubeluzole	3.69	210	1	0.29	1748.06	1000.20	100
8	3.28	130	1	0.11	613.96	1032.00	100
15g	3.91	280	1	0.40	2944.29	1354.03	100
15h	4.59	276	2	0.68	9123.66	1354.13	96.92
15i	3.16	299	1	−0.12	845.09	426.66	92.52
15l	3.32	162	1	0.04	614.05	1032.12	100
15m	3.53	205	1	0.13	999.93	1354.24	100
16n	2.58	174	1	−0.48	176.22	325.20	87.01
16o	2.02	220	−1	−0.94	79.61	130.30	76.65

+2 (active); (ii) QPlogBB, estimating the brain/blood partition coefficient; (iii) QPPMDCK, estimating MDCK cell permeability (considered a good mimic for the blood-brain barrier) in nm/sec (<25 poor, >500 great); (iv) QPPCaco, estimating Caco-2 cell permeability in nm/sec (i.e., ability to cross the gut-blood barrier; <25 poor, >500 great); (v) PercentHumanOralAbsorption, providing a score based on multiple

linear regression on a scale from 0 to 100% (>80% is high, <20% is poor). From the data reported for these parameters, it is evident that all the compounds under investigation are predicted to exhibit good oral absorption. Regarding the ability to cross the blood-brain barrier and act at the CNS level, all the compounds, with the exception of **16o** returning a negative CNS value (−1) and a QPlogBB value of −0.94, are predicted to affect the CNS. In summary, the analysis of the predicted properties of the synthesized compounds suggests **16o** as the most promising candidate. However, the predicted hERG blocker ability, reported as IC_{50} (QPIC50HERG parameter) is fairly similar among them, indicating the need for experimental assessment of all compounds' ability to block hERG channels.

2.3. hERG binding activity

All the synthesized compounds (**8**, **15g–m** and **16n,o**) were tested in vitro to investigate their effect on hERG potassium channels. Patch-clamp experiments were performed on HEK cells heterologously expressing the hERG channel (Fig. 2) and the results are reported in Table 2. Based on the lack of stereoselectivity showed by lubeluzole (Table 2), as previously described [4], all the analogues were prepared in racemic form.

Compound **8** was significantly more potent than lubeluzole in inhibiting the hERG channel, thus indicating that the presence of the two fluorine atoms on the phenoxy moiety is detrimental to the binding capacity of the ligand.

Starting from the consideration that, although both 1,3-benzothiazole-2-amine and 3-aryloxy-2-propanolamine moieties of lubeluzole may contribute to hERG binding, the former seems to give a higher contribution [4], stereoelectronic effects of substituents on the 6-benzothiazole position were first investigated (compounds **15g–i**). The electron-withdrawing CF_3 group (**15h**) increased potency by an order of magnitude in comparison to lubeluzole, also corroborating the well-known relationship between lipophilicity and hERG liability [19]. On the contrary, compounds **15g** and **15i** behave like the parent compound (**15f**), thus suggesting that the presence of one electron-donating group, acting as hydrogen bond acceptor (HBA) (**15g**) or as both HBA and HB donor (HBD) (**15i**), on the benzothiazole ring (R^3) does not affect channel binding capacity.

To further reduce the overall compound lipophilicity, analogues bearing polar substituents on the aryloxy moiety in place of fluorine atoms were also designed. In particular, with the aim of identifying lubeluzole analogues as potent voltage-gated sodium channel blockers endowed with reduced affinity for the hERG channel, we got inspiration from a peculiar effect of regioselective hydroxylation of the xylyl ring of mexiletine, a known sodium channel blocking agent commonly used as an antiarrhythmic [22] and antimyotonic drug [23]. Unlike variously hydroxylated mexiletine analogues less potent than the parent compound [24], the so-called *meta*-hydroxymexiletine, bearing a hydroxyl group in the 3-position of the aromatic ring, kept the same biological activity [25] showing, however, reduced potency on hERG [26] with respect to the parent compound. Summing these findings, the variously oxygenated congeners of lubeluzole **15l,m** and **16n,o** were also prepared.

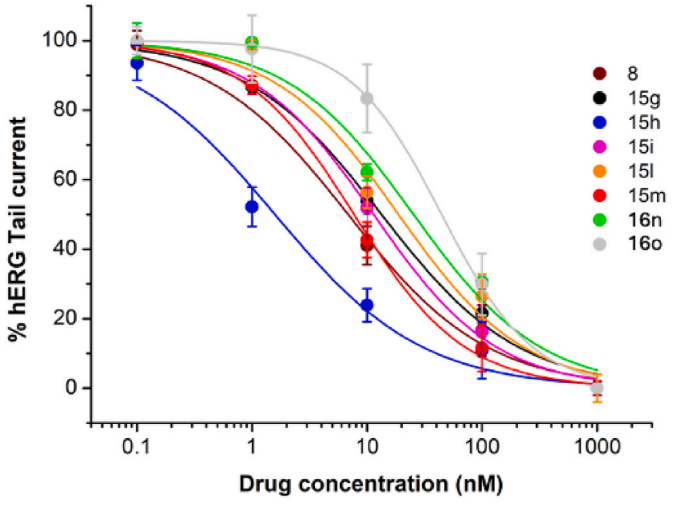

Fig. 2. Effects of lubeluzole analogues on hERG tail current (mean ± SEM, $n \geq 5$ per data point). A Hill equation fit yielded the IC_{50} and Hill slope (n_H) values shown in Table 2.

Table 2
hERG channel inhibition displayed by lubeluzole (**15f**) and its analogues (**8**, **15g–m**, and **16n,o**).

Compd.	IC_{50} (nM)	n_H
(*RS*)-lubeluzole[a]	11.1 ± 0.4	1.10 ± 0.03
lubeluzole (**15f**)	12.9 ± 0.7	0.84 ± 0.05
8	6.8 ± 1.7	0.72 ± 0.13
15g	13.3 ± 1.9	0.73 ± 0.07
15h	1.5 ± 0.4	0.68 ± 0.12
15i	11.4 ± 1.4	0.82 ± 0.09
15l	18.8 ± 5.4	0.80 ± 0.16
15m	7.7 ± 0.7	0.90 ± 0.06
16n	25.3 ± 7.0	0.79 ± 0.15
16o	44.5 ± 3.2	1.10 ± 0.07

[a] Ref. [4].

The replacement of both aryloxy fluorine atoms with a group containing an oxygen atom in the 3-position (**15l** and **16n**) did not significantly affect the potency in comparison with lubeluzole. In general, it would seem that steric effects at the aryloxy moiety have higher leverage than electronic effects in the interaction with the channel. Surprisingly, compound **15m** was as potent as the analogue **8**, thus indicating that the absence of substituents (**8**), as well as the presence of HBA groups on both the aromatic moieties of lubeluzole (**15m**), ensure high affinity for the channel. Finally, interesting results were obtained for the dihydroxylated analogue **16o** which was about 4-fold less active than the reference compound. These results prompted us to consider **16o** as the most promising compound possibly endowed with a lower cardiac liability, thus being worthy of further pharmacological investigations.

2.4. Voltage-gated sodium channel blocking activity

Compound **16o** was tested on sodium currents recorded in HEK293 cells expressing the human skeletal muscle hNav1.4 voltage-gated sodium channel, and lubeluzole (**15f**) was used as the reference compound. The currents were elicited by depolarizing the cell membrane from −120 to −30 mV at two stimulation frequencies, 0.1 and 10 Hz, to determine both tonic and phasic blocks, respectively. The effects of both compounds on tonic and phasic blocks of hNav1.4 are shown in Fig. 3 and the IC_{50} values are reported in Table 3.

The results suggest that the affinity of **16o** to hNav1.4 channels is slightly reduced compared to that of lubeluzole. The reduction is more evident at 0.1 Hz stimulation frequency, which is in accord with the reduced lipophilia of **16o** that may reduce access to the binding site within the closed channel. The affinity to inactivated channels is less affected by **16o** chemical modifications. Thus, **16o** showed an increased IC_{50} ratio between 0.1 and 10 Hz, which may favor its selectivity toward highly excited tissues, such as the myotonic muscle.

Being known that lubeluzole also blocks cardiomyocytes' voltage-gated sodium channels [27], compound **16o** was tested on cardiac hNav1.5 sodium currents (Fig. 4 and Table 3) to evaluate a possible sodium channel isoform selectivity in support of a further reduced cardiac liability. It was about 3-fold less potent on hNav1.5 than hNav1.4 in phasic block (IC_{50} values 12 ± 2 and 4.4 ± 0.6 μM, respectively) and showed a TB/PB ratio on Nav1.5 higher than lubeluzole, thus suggesting

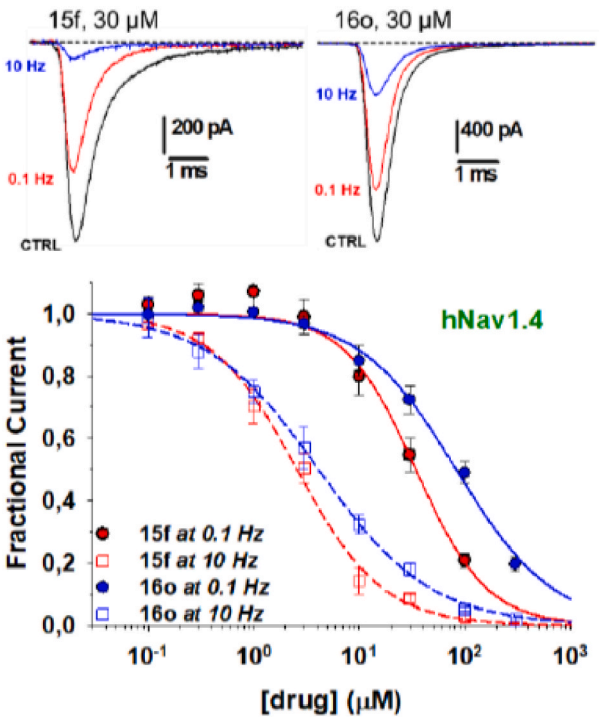

Fig. 3. Effects of lubeluzole (**15f**) and its dihydroxy analogue **16o** on skeletal muscle hNav1.4 sodium channels expressed in HEK cells. Upper panel: sodium currents were elicited by voltage pulses from the holding membrane potential of −120 mV to −30 mV before (CTRL) and after application of the drug at 0.1 Hz then 10 Hz frequency stimulation. Lower panel: the concentration/response curves were constructed at 0.1 and 10 Hz. Each data point is the mean ± SEM from 3 to 9 cells. The relationships were fit with standard Hill equation $I_{DRUG}/I_{CTRL} = 1/(1+[DRUG]/IC_{50})$, where IC_{50} (µM) is the half-maximum inhibitory concentration and h is the logistic slope factor.

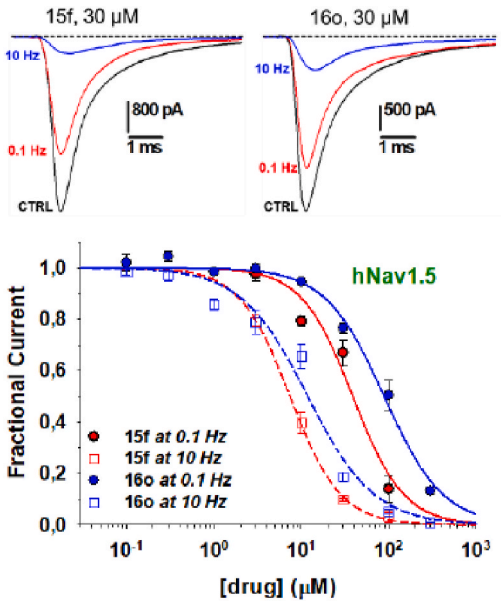

Fig. 4. Effects of lubeluzole (**15f**) and its dihydroxy analogue **16o** on cardiac hNav1.5 sodium channels expressed in HEK cells. Upper panel: sodium currents were elicited by voltage pulses from the holding membrane potential of −120 mV to −30 mV before (CTRL) and after application of the drug at 0.1 Hz then 10 Hz frequency stimulation. Lower panel: the concentration/response curves were constructed at 0.1 and 10 Hz. Each data point is the mean ± SEM from 3 to 9 cells. The relationships were fit with standard Hill equation $I_{DRUG}/I_{CTRL} = 1/(1+[DRUG]/IC_{50})^h$, where IC_{50} (µM) is the half-maximum inhibitory concentration and h is the logistic slope factor.

a predominant effect on the muscular tissue greater than that of lubeluzole. In other words, based on the results obtained on both Nav1.5 and hERG channels, we can speculate that the dihydroxy analogue **16o** may act less than lubeluzole on the heart when used as an antimyotonic agent. On the other hand, a residual blocking activity on cardiac sodium channels might be beneficial when long QT syndrome is feared [28].

These findings prompted us to evaluate a possible in vivo antimyotonic effect of compound **16o**, using lubeluzole as the reference compound. The reduction of the time of righting reflex in vivo in the rat model of myotonia was observed (Fig. 5). In this model, myotonia is induced in adult rats by a single intraperitoneal injection of 9-anthracenecarboxylic acid (9-AC). By blocking muscle ClC-1 chloride channels, 9-AC induces a myotonic state similar to that observed in Myotonia Congenita. The myotonic state can be evaluated by measuring the time of righting reflex (TRR), that is the time taken by the rat to turn back on his four limbs after being posted in the supine position [29,30].

Lubeluzole was very efficient in reducing TRR, thus confirming previous data. Very surprisingly, compound **16o** induced a huge increase in the TRR, suggesting unexpected side effects on rat motor performance. Starting from the consideration that a parabolic relationship between lipophilicity and CNS bioavailability is now well-established, we hypothesized a possible higher CNS penetration of **16o** than the more lipophilic lubeluzole. The ability of lubeluzole and compound **16o** to cross the blood-brain barrier (BBB) was assessed using a Caco-2 cell monolayer model overexpressing human P-glycoprotein (P-gp), a widely accepted in vitro system for predicting BBB permeability [31]. Transport was measured in both basolateral-to-apical (BA) and apical-to-basolateral (AB) directions. Since efflux pumps such as P-gp are localized on the apical side, the BA direction primarily reflects passive diffusion, whereas the AB direction is influenced by active efflux mechanisms. Lubeluzole and **16o** showed high passive permeability, with PappBA values of 2047 and 2402 nm/s, respectively. However, transport was significantly reduced for both compounds in the AB direction, with PappAB values of just 292 nm/s. The resulting BA/AB ratios of 7.0 for lubeluzole and 8.2 for **16o** clearly indicate strong efflux activity. These findings suggest that, although both compounds can diffuse passively, they are efficiently recognized and transported out by P-gp, limiting their accumulation beyond the BBB.

2.5. Peripheral off-target activities

To verify the possibility that the adverse effects displayed in vivo by **16o** could stem from peripheral off-target activities, the affinity of lubeluzole and **16o** on α_{1A} and β_2 receptors was then evaluated and, although no differences were observed on α_1, **16o** was significantly more potent than lubeluzole on β_2 receptors (Table 4). A β-blocker activity might directly reduce skeletal muscle function, including a counterproductive slowing of muscle relaxation [32]. In addition, β-blocking might reduce skeletal muscle oxygenation through local blood flow reduction (vasocontriction of skeletal muscle arteries) and broncoconstriction [33].

In a previous study, we demonstrated a spasmolytic effect of lubeluzole on rat colon and relaxant activity on guinea pig gut tissues, maybe in relation to L-type calcium channel inhibition [7]. Thus, we investigated the effects of **16o** on high potassium-induced contractility in guinea pig ileum longitudinal smooth muscle [34,35]. Regardless of the tissue being studied, this assay indirectly provides information about the ability of the tested compounds to interfere with the movement of calcium through voltage-gated channels [36]. Both lubeluzole and **16o** displayed a dose-dependent relaxing effect depicted in Fig. 6 but, as reported in Table 5, **16o** was significantly more potent than lubeluzole. Thus, **16o** might impair calcium homeostasis in excitable tissues, thereby interfering with muscle function

Summing up these findings, the unwanted peripheral effects of **16o**

Table 3
Half-maximum inhibitory concentrations of lubeluzole (**15f**) and its dihydroxy analogue **16o** on sodium channels.

Compd.	channel	0.1 Hz		10 Hz		0.1- to 10-Hz IC_{50} ratio
		IC_{50} (μM)	h	IC_{50} (μM)	h	
lubeluzole (**15f**)	hNav1.4	34 ± 4	1.3 ± 0.2	2.6 ± 0.2	1.1 ± 0.1	13.1
	hNav1.5	37 ± 8	1.7 ± 0.6	7.0 ± 0.1	1.6 ± 0.1	5.3
16o	hNav1.4	83 ± 6	1.0 ± 0.1	4.4 ± 0.6	0.7 ± 0.1	18.9
	hNav1.5	88 ± 7	1.3 ± 0.1	12 ± 2	1.2 ± 0.2	7.3

The concentration-response relationships in Figs. 3 and 4 were fit with standard Hill equation $I_{DRUG}/I_{CTRL} = 1/(1+[DRUG]/IC_{50})^h$, where IC_{50} (μM) is the half-maximum inhibitory concentration and h is the logistic slope factor. Each value is reported with the S.E. of the fit.

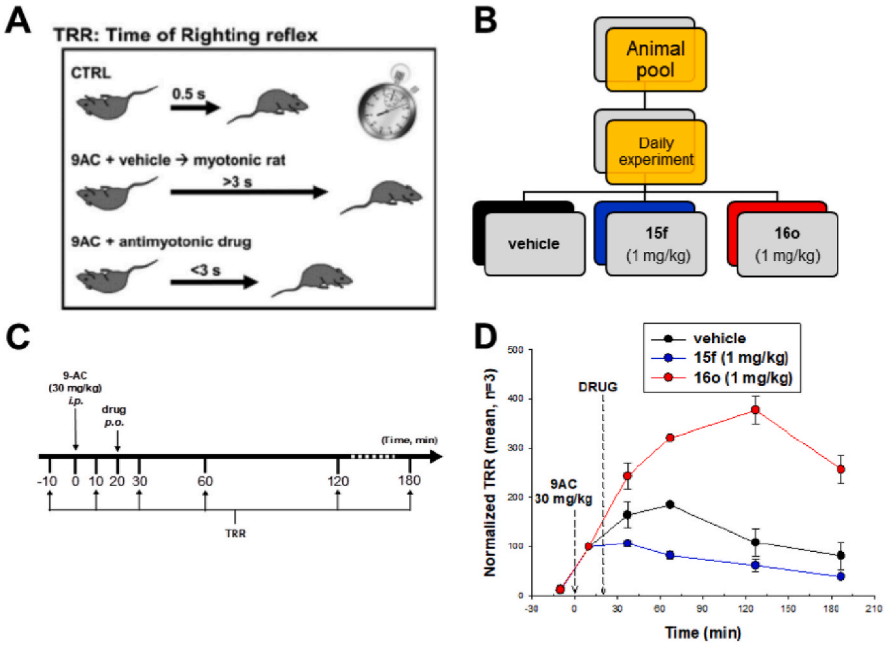

Fig. 5. **(A)** Time of righting reflex (TRR). After i.p. injection of 9-AC, a chloride channel blocker, the TRR is lengthened by more than 3 s. In the presence of a putative antimyotonic drug (oral administration), the TTR is reduced to less than 3 s. **(B)** Organization of a daily experiment. **(C)** Study protocol. The TRR is measured 10 min before and 10, 30, 60, and 120 min after 9-AC administration. The exploratory drug is given 20 min after 9-AC. **(D)** Time course of TRR value after oral injection of vehicle, lubeluzole (1 mg/kg), or **16o** (1 mg/kg).

Table 4
Affinity of lubeluzole and **16o** on α_{1A} and β_2 receptors.

Compd.	K_i (nM ± S.E.M.)	
	α_{1A}	β_2
lubeluzole (**15f**)	180 ± 40 (n = 3)	190 ± 70 (n = 4)
16o	270 ± 60 (n = 3)	14 ± 2.9 (n = 4)

should be related to its aryloxy propanolamine scaffold (general β-blocker structure). In principle, the off-target interaction with β-receptors might be easily reduced in properly designed upcoming analogues. Starting from the consideration that no stereoselectivity was observed for lubeluzole on both voltage-gated sodium and hERG channels, it is reasonable to assume that the hydroxyl group attached to the asymmetric carbon is not a major pharmacophoric element for both targets; thus, it could be formally removed to avoid the putative β-blocker behaviour. As regards the possibility of preventing a putative residual β-agonist activity, knowing that the hydroxyl in the 3-aryloxy position plays a pivotal role in the β-agonist behaviour, novel analogues of **16o** bearing bulky hydroxyalkyl groups in place of the phenolic hydroxyl could be prepared to investigate the optimal alkyl chain length possibly leading to loss of a possible intrinsic sympathomimetic activity while keeping under control hERG affinity.

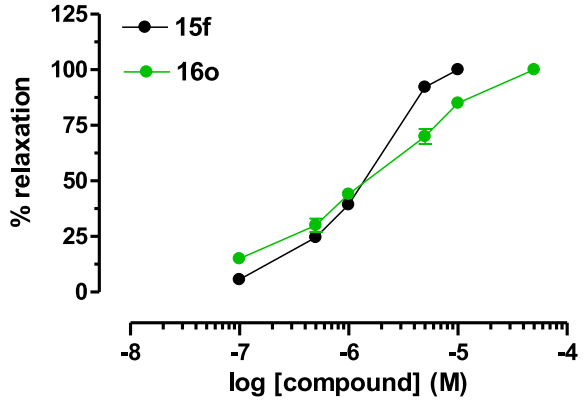

Fig. 6. Cumulative concentration-response curves for lubeluzole (**15f**) (black) and **16o** (green) on K^+-depolarized guinea pig ileum longitudinal smooth muscle. Each point is the mean ± SEM of four-six experiments. Where error bars are not shown these are covered by the point itself. (For interpretation of the references to color in this figure legend, the reader is referred to the Web version of this article.)

Table 5
Relaxant activity of the tested compounds on K^+-depolarized guinea pig longitudinal ileum smooth muscle.

Compd.	IA[a] (M ± SEM)	IC_{50}[b] (μM)	95% conf lim (x10^{-6})
lubeluzole (**15f**)	90 ± 1.6	1.40	1.10–1.80
16o	89 ± 0.4	0.83	0.47–1.03

[a] IA (Intrinsic Activity), expressed as percent inhibition of calcium-induced contraction on K^+-depolarized (80 mM) guinea pig ileum longitudinal smooth muscle at 10^{-5} M.
[b] Calculated from log concentration-response curves (Probit analysis by Litchfield and Wilcoxon [37] with $n = 6–7$).

2.6. Molecular modelling

Once a large panel of affinities and activities was acquired, we investigated **16o** in a three-dimensional perspective of its structural chemical properties by modelling the interaction with a properly selected target, and to attempt this task, molecular docking to the β-adrenoceptor was indeed performed. To get insights into the plausible binding mode, the long-acting agonist olodaterol crystallized with the human β_2-adrenergic receptor was taken as reference compound to assess the **16o** binding pose. Docking results (Fig. 7) showed a clear interaction pattern of our ligand with the seven transmembrane binding cleft of the receptor, since the charged nitrogen of the piperidine ring is anchoring the binder to the third transmembrane helix, strongly interacting with Asp113, and simultaneously the hydroxyl group recruits Tyr334 with a direct hydrogen bond. Moreover, the aryloxy moiety is pointing towards the vestibular entry cavity where three residues, namely His93, Phe193, and Lys372, stabilize the binding through both polar and hydrophobic interactions, and very importantly, the benzothiazole scaffold generates *edge-to-face* π−π stackings with the fully conserved and constitutively essential aromatic cluster defined by Trp353, Phe356, and Phe357 as located in the sixth transmembrane segment. As additional help, Thr118 and Ser207 get hydrogen bonds with the 6-OH group of **16o**. All the mentioned residues have been highlighted as essential from site-directed mutagenesis data [38], but also dockings were indeed corroborated with scores reported in Table 6.

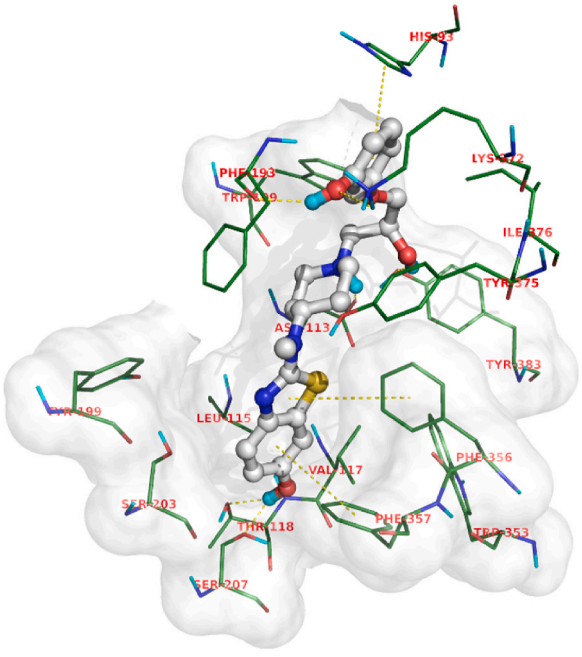

Fig. 7. Binding mode of **16o** to the β_2 active site. For sake of clarity, the hydrogen bonds and π-π stackings are depicted as yellow dashed lines. (For interpretation of the references to color in this figure legend, the reader is referred to the Web version of this article.)

The above table referred to what is proposed by us as screening rule named **ESP**, applied to rank binding poses according to more than one filtering figures, namely energy (**E**), similarity (**S**) and population (P), and the rule is valid once at least four out of five parameters are below certain thresholds (see methods). It has to be pointed out that no significant differences in the binding mode of **16o** were detected between the two enantiomeric forms.

According to this additional evidence, our original hypothesis regarding the **16o** plausible role in the downregulation and β_2-adrenoceptor mediated off-target activities was further validated.

3. Conclusions

A series of lubeluzole analogues have been prepared and their effect on hERG potassium channels was preliminarily evaluated, thus identifying compound **16o** as the less potent hERG blocker possibly endowed with a lower cardiac liability in comparison with the parent compound. In silico profiling of relevant pharmacokinetic properties suggested **16o** as the most promising candidate for oral absorption, also possibly endowed with poor central side effects. The latter property was confirmed by evaluation of **16o** permeability across an epithelial colorectal adenocarcinoma (Caco-2) cell monolayer. Antimyotonic activity of **16o** was therefore in vitro evaluated on hNav1.4 and higher use-dependence than lubeluzole was observed, thus suggesting greater selectivity toward highly excited tissues, such as the myotonic muscle. The presumed reduced cardiac liability of **16o** was corroborated by 3-fold reduced potency on hNav1.5 compared to hNav1.4 in the phasic block, with higher use-dependence on cardiac tissue than lubeluzole. The in vivo evaluation in the rat model of myotonia showed unexpected side effects on rat motor performance, which might rely on off-target effects on β_2 adrenoceptors and voltage-gated calcium channels. The affinity towards the β_2-adrenergic receptor was supported by docking and affinity assays, without any functional validation; therefore, the physiological relevance of this interaction needs more in-depth investigations. On the other hand, since the calcium channel blocking activity was evaluated through ex vivo studies, providing a preliminary indication without a detailed mechanistic characterization, electrophysiological experiments are required to confirm this effect. The obtained results pave the way for more in-depth studies devoted to identifying safer lubeluzole analogues useful in treating myotonia.

4. Experimental section

4.1. Chemistry

4.1.1. General

Chemicals were purchased from Merck or Alfa Aesar in the highest quality commercially available. Solvents were RP grade unless otherwise indicated. Commercially available benzothiazole was used to prepare lubeluzole. Compounds **14c–e** were synthesized, although commercially available, and only spectrometric analyses were

Table 6
Summary of the docking results.

	FEB[a]	ΔE[b]	EFF[c]	TAN[d]	POP[e]
(*R*)-16o	−12.22	0.00	−0.407	0.532	25/1000
(*S*)-16o	−12.46	0.00	−0.415	0.477	276/1000
olodaterol	−13.52	0.00	−0.483	1.042	211/1000

[a] **FEB** Free Energy of Binding.
[b] **ΔE** Energy difference between the selected pose and the relative global minimum.
[c] **EFF** Ligand efficacy.
[d] **TAN** Tanimoto similarity coefficient with olodaterol binding pose.
[e] **POP** Cluster members population.

performed. Yields refer to purified products and were not optimized. Routine spectrometric analyses confirmed the structures of the compounds. Compound **5** was prepared as previously described [11] (Chirality2006) and only spectra for compounds not previously described are given. Melting points were determined on a Gallenkamp melting point apparatus in open glass capillary tubes and are uncorrected. ^{1}H NMR and ^{13}C NMR spectra were recorded on either a Varian VX Mercury spectrometer operating at 300 and 75 MHz for ^{1}H and ^{13}C, respectively, or an Agilent 500 MHz operating at 500 and 125 MHz for ^{1}H and ^{13}C, respectively, using $CDCl_3$ as solvent, unless otherwise indicated. Chemical shifts are reported in ppm relative to the residual non-deuterated solvent resonance: $CDCl_3$, δ 7.26 (^{1}H NMR) and δ 77.3 (^{13}C NMR). *J* values are given in Hertz. Electron ionization mass spectroscopy spectra were recorded on a Hewlett–Packard 6890–5973 MSD gas chromatograph/mass spectrometer at low resolution. The molecular ion is given as $[M]^+$. Elemental analyses were performed on a Eurovector Euro EA 3000 analyzer, and the data for C, H, and N were within ±0.4 of theoretical values. Chromatographic separations were performed on silica gel columns (Kieselgel 60, 0.040–0.063 mm, Merck). Thin layer chromatography (TLC) analyses were performed on precoated silica gel on aluminum sheets (Kieselgel 60 F254, Merck). TLC plates were visualized under UV light. The purity of the final compounds was determined by elemental analysis.

*4.1.1.1. 2-[(Phenoxy)methyl]oxirane (RS)-**7**.* A solution of NaOH (1.31 g, 32.8 mmol) in 37 mL of water was added dropwise to a mixture of phenol (**6**, 3.00 g, 31.9 mmol) and (*RS*)-epichlorohydrin (2.98 mL, 38.3 mmol). The reaction mixture was refluxed for 3 h and then extracted with EtOAc. The combined organic layers were dried over anhydrous Na_2SO_4 and the solvent was removed in vacuo. The residue was purified by flash chromatography (1:10 EtOAc/hexane) to give 2.85 g of (*RS*)-**7** as a colorless oil (60%): GC–MS (70eV) *m/z* (%) 150 (M^+, 100). Spectroscopic data were in agreement with those reported in the literature [39].

*4.1.1.2. (RS)-1-{4-[1,3-Benzothiazol-2-yl(methyl)amino]piperidin-1-yl}-3-phenoxypropan-2-ol [(RS)-**8**].* A solution of the epoxide (*RS*)-**7** (0.11 g, 0.7 mmol) in dry CH_2Cl_2 (1.7 mL) was treated with the amine **5** (0.22 g, 0.9 mmol) and $Yb(OTf)_3$ (50 mg, 10% mol) and the reaction mixture was stirred at room temperature for 6 h. After evaporation of the solvent, the residue was taken up with EtOAc, in turn washed with brine, dried over anhydrous Na_2SO_4, and concentrated in vacuo. The crude product was purified by flash chromatography (9.5:0.5 EtOAc/MeOH) to give 0.20 g (72%) of the desired (*RS*)-**8** as a yellowish oil; HRMS *m/z* calcd for $C_{22}H_{28}N_3O_2S$: 398.1897 ($[M + H]^+$); found 398.1907. The corresponding hydrochloride [(*RS*)-**8**·HCl] was obtained by dissolving the free base in anhydrous Et_2O and treating with gaseous HCl for a few seconds. Yield: 48%; mp 190–192 °C (abs EtOH/Et_2O); ^{1}H NMR (300 MHz, CD_3OD): δ 2.20–2.42 (m, 2H), 2.44–2.56 (m, 2H), 3.34 (apparent s, 5H), 3.38–3.54 (m, 4H), 3.85–3.98 (m, 2H), 4.00 (t overlapping m at 3.98–4.10, *J* = 5.2 Hz, 1H), 3.98–4.10 (m overlapping t at 4.00, 1H), 4.42–4.54 (m, 2H), 6.90–7.02 (m, 3H), 7.28 (dd, *J* = 8.7, 7.3 Hz, 2H), 7.41 (t, *J* = 8.2 Hz, 1H), 7.56 (t, *J* = 7.3 Hz, 1H), 7.68 (d, *J* = 8.0 Hz, 1H), 7.88 (d, *J* = 8.0 Hz, 1H); ^{13}C NMR (125 MHz, CD_3OD): 25.5 (2C), 33.4 (1C), 50.7 (1C), 52.8 (2C), 59.2 (1C), 64.0 (1C), 69.6 (1C), 114.2 (2C), 114.4 (1C), 120.9 (1C), 122.4 (1C), 123.4 (1C), 124.8 (1C), 128.0 (1C), 129.2 (2C), 139.6 (1C), 158.4 (1C), 168.9 (1C). Anal. Calcd for ($C_{22}H_{27}N_3O_2S$·2HCl·H_2O): C, 54.09; H, 6.40; N, 8.60; Found: C, 54.37; H, 6.65; N, 8.58.

*4.1.1.3. 2-[(3,4-Difluorophenoxy)methyl]oxirane [(RS)-**10a**].* Prepared as previously reported. Spectrometric and spectroscopic data were in agreement with those reported in the literature [11,14].

*4.1.1.4. 2-[(3-Methoxyphenoxy)methyl]oxirane [(RS)-**10b**].* To a stirred solution of 3-methoxyphenol (**9b**) (3.0 g, 24.2 mmol) in acetonitrile (50 mL) (*RS*)-epichlorohydrin (7.5 mL, 96.8 mmol) and Cs_2CO_3 (15.8 g, 48.4 mmol) were added. The reaction mixture was refluxed for 17 h, then filtered through a Celite pad, in turn washed with EtOAc, and concentrated under reduced pressure to afford the crude product purified by flash chromatography (EtOAc/hexane, 9:1). Compound (*RS*)-**10b** was obtained as a colorless oil (3.58 g, 82%); GC–MS (70eV) *m/z* (%) 180 (M^+, 100). Spectroscopic data were in agreement with those reported in the literature [40].

*4.1.1.5. General procedure for the synthesis of compounds (RS)-**11a,b**.* The method adopted for the synthesis of (*RS*)-1-[3-(3,4-difluorophenoxy)-2-hydroxypropyl]piperidin-4-one [(*RS*)-**11a**] is described.

A solution of [(3,4-difluorophenoxy)methyl]oxirane [(*RS*)-**10a**] (0.50 g, 2.7 mmol) and piperidine-4-one (0.802 g, 8.2 mmol) in dichloromethane (5 mL) was stirred for 8 min at 100 °C in a microwave reactor under continuous stirring. When the reaction was completed, the solvent was removed under vacuum and the residue was taken up with EtOAc, in turn extracted with 2 M HCl. The combined aqueous phases were made alkaline with 6 M NaOH and extracted with EtOAc, then dried over anhydrous Na_2SO_4, and concentrated in vacuo to give 0.445 g of a yellow oil (58%): GC–MS (70eV) *m/z* (%) 285 (M^+, <1); 112 (100). Spectroscopic data are in agreement with those reported in the literature [41].

*4.1.1.6. (RS)-1-[2-Hydroxy-3-(3-methoxyphenoxy)propyl]piperidin-4-one [(RS)-**11b**].* The title compound was prepared starting from (*RS*)-**10b** and stirring the reaction mixture for 12 min: Yield 90% (orange oil); IR (neat)**:** 3416 (OH), 1715 (CO) cm^{-1}; GC–MS (70eV) *m/z* (%) 279 (M^+, 2), 112 (100); ^{1}H NMR (500 MHz): δ 2.40 (t, *J* = 6.2 Hz, 1H), 2.43–2.53 (m, 4H), 2.64–2.72 (m, 2H), 2.77–2.84 (m, 1H), 2.94–3.00 (m, 1H), 3.14 (t, *J* = 6.4 Hz, 1H), 3.77 (br s, exch. D_2O, 1H), 3.78 (s, 3H), 3.99–4.01 (m, 2H), 4.08–4.15 (m, 1H), 6.46–6.54 (m, 3H), 7.18 (apparent t, 1H); ^{13}C NMR (125 MHz): 41.1 (2C), 43.6 (1C), 47.1 (1C), 55.3 (1C), 59.5 (1C), 66.4 (1C), 70.1 (1C), 101.1 (1C), 106.6 (1C), 106.7 (1C), 129.9 (1C), 159.8 (1C), 160.8 (1C), 208.3 (1C).

*4.1.1.7. General procedure for the synthesis of compounds (RS)-**12a,b**.* The method adopted for the synthesis of (*RS*)-1-(3,4-difluorophenoxy)-3-[4-(methylamino)piperidin-1-yl]propan-2-ol [(*RS*)-**12a**] is described.

A mixture of (*RS*)-1-[3-(3,4-difluorophenoxy)-2-hydroxypropyl] piperidin-4-one [(*RS*)-**11a**] (0.50 g, 1.8 mmol), methylamine hydrochloride (1.20 g, 18 mmol), and $NaBH_3CN$ (0.079 g, 1.26 mmol) in MeOH (3 mL) was stirred for 11 min at 110 °C in a microwave reactor under continuous stirring. When the reaction was completed, 6 M HCl was added dropwise until effervescence is not longer observed. After evaporation of the solvent, the residue was taken up with H_2O which was washed with Et_2O, made alkaline with 2 M NaOH, and extracted with Et_2O. The combined organic phases were dried over anhydrous Na_2SO_4, and concentrated in vacuo to give 1.06 g of a yellow oil (87%). GC–MS (70eV) *m/z* (%) 271 ($M^+ - 29$, <1); 84 (100). Spectroscopic data are in agreement with those reported in the literature [41].

*4.1.1.8. (RS)-1-(3-Methoxyphenoxy)-3-[4-(methylamino)piperidin-1-yl] propan-2-ol [(RS)-**12b**].* The title compound was prepared starting from (*RS*)-**11b**: Yield: 74%; IR (neat): 3306 (OH + NH) cm^{-1}; GC–MS (70eV) *m/z* (%) 280 ($M^+ - 14$, 2), 84 (100); ^{1}H NMR (500 MHz): δ 1.30–1.44 (m, 2H), 1.86–1.92 (m, 2H), 2.07 (dt, *J* = 11.2, 2.5 Hz, 1H), 2.35 (dt, *J* = 11.2, 2.4 Hz, 1H), 2.37–2.41 (m, 1H), 2.43 (s, 3H), 2.49 (dd, *J* = 12.5, 4.2 Hz, 1H), 2.54 (dd, *J* = 12.5, 9.5 Hz, 1H), 2.80–2.85 (m, 1H), 2.96–3.02 (m, 1H), 3.78 (s, 3H), 3.96 (d, *J* = 5.4 Hz, 2H), 4.04–4.10 (m, 1H), 6.48–6.54 (m, 3H), 7.17 (apparent t, 1H); ^{13}C NMR (125 MHz): 32.3 (1C), 32.5 (1C), 33.4 (1C), 51.5 (1C), 53.7 (1C), 55.2 (1C), 56.3 (1C), 60.5 (1C), 65.7 (1C), 70.5 (1C), 101.2 (1C), 106.67 (1C), 106.73 (1C), 129.8 (1C), 160.1 (1C), 160.9 (1C).

*4.1.1.9. 2-Chloro-6-methoxy-1,3-benzothiazole (**14c**).* To an ice-cold solution of $CuCl_2$ (3.47 g, 20.4 mmol) and *tert*-butyl nitrite (3 mL) in acetonitrile (120 mL) 2-amino-6-methoxy-1,3-benzothiazole (**13c**) (3.0 g, 16.7 mmol) was added in six portions at 15-min intervals and the reaction mixture was stirred at room temperature for 2 h, then at 70 °C for 1 h. The solid was filtered off and the filtrate was poured into 6 M HCl, extracted with EtOAc, in turn washed with brine. The combined organic phases were dried over anhydrous Na_2SO_4, and concentrated in vacuo to give 3.29 g of a brown solid (99%). Mp 81–82 °C; GC–MS (70eV) *m/z* (%) 199 (M^+, 100). Spectroscopic data were in agreement with those reported in the literature [42].

*4.1.1.10. 2-Chloro-6-(trifluoromethyl)-1,3-benzothiazole (**14d**).* A mixture of $CuCl_2$ (0.491 g, 2.89 mmol) and *tert*-butyl nitrite (0.371 g, 3.60 mmol) in acetonitrile (5 mL) was stirred at room temperature for 10 min, then a solution of 2-amino-6-trifluoromethyl-1,3-benzothiazole (**13d**) (0.445 g, 2.04 mmol) in acetonitrile (1 mL) was added dropwise. The reaction mixture was refluxed at 70 °C for 30 min, returned to room temperature, and then poured into 6 M HCl. The aqueous phase was extracted with EtOAc, in turn washed with brine. The combined organic phases were dried over anhydrous Na_2SO_4, and concentrated in vacuo to give 0.460 g of an orange solid (95%): GC–MS (70eV) *m/z* (%) 237 (M^+, 100). Spectroscopic data were in agreement with those reported in the literature [43,44].

*4.1.1.11. 2-Chloro-6-hydroxy-1,3-benzothiazole (**14e**).* Aluminum chloride (1.86 g, 14.06 mmol) was added to a solution of 2-chloro-6-methoxy-1,3-benzothiazole (**14c**) (1.0 g, 5.02 mmol) in toluene (40 mL) and the mixture was heated at 110 °C for 1 h. The reaction mixture was cooled to room temperature and 1 M HCl was added. The precipitate was collected by filtration, washed with water, then with $NaHCO_3$ saturated solution, and air-dried to give the desired product (0.654 g) as a brown solid. Toluene, separated from the acidic aqueous phase using a separatory funnel, was dried over anhydrous Na_2SO_4, and concentrated in vacuo giving 0.275 g of the desired product (quantitative overall yield): GC–MS (70eV) *m/z* (%) 185 (M^+, 100). Spectroscopic data were in agreement with those reported in the literature [45].

*4.1.1.12. General procedure for synthesizing compounds (RS)-**15f–m**.* The method adopted for the synthesis of (*RS*)-1-{4-[1,3-benzothiazol-2-yl(methyl)amino]piperidin-1-yl}-3-(3,4-difluorophenoxy)propan-2-ol [(*RS*)-**15f**, lubeluzole] is described.

A solution of (*RS*)-1-(3,4-difluorophenoxy)-3-[4-(methylamino) piperidin-1-yl]propan-2-ol [(*RS*)-**12a**] (0.360 g, 1.19 mmol), 2-chlorobenzothiazole (0.304 g, 1.79 mmol), and TEA (183 μL) in water (2 mL) was kept under reflux for 10 h. The mixture was brought to room temperature and taken up with H_2O which was in turn extracted with EtOAc. The combined organic layers were dried over Na_2SO_4 and concentrated under vacuum to give 0.918 g of an orange oil purified by flash chromatography (EtOAc, then EtOAc/MeOH 9.5:0.5) to give 0.440 g of a colorless oil. Spectrometric and spectroscopic data were in agreement with those reported in the literature [11]. (*RS*)-**15f**·HCl was obtained by treating the free base with a few drops of hydrochloric aqueous solution and removing water by azeotropic distillation (abs EtOH/toluene). The obtained white solid was recrystallized from $CHCl_3$/abs EtOH/hexane to give 0.315 g of white crystals. Yield: 85%; mp 228–230 °C ($CHCl_3$/abs EtOH/hexane); Anal. Calcd for $C_{22}H_{25}F_2N_3O_2S{\cdot}2HCl$: C, 52.18; H, 5.37; N, 8.30. Found: C, 52.24; H, 5.39; N, 8.33. Spectrometric and spectroscopic data were in agreement with those reported in the literature [11].

*4.1.1.13. (RS)-1-{4-[6-Methoxy-1,3-benzothiazol-2-yl(methyl)amino] piperidin-1-yl}-3-(3,4-difluorophenoxy)propan-2-ol [(RS)-**15g**].* The title compound was prepared starting from (*RS*)-**12a** and **14c**: Yield: 35%; IR (neat): 3335 (OH) cm^{-1}; ESI^+/MS: 486 (M^+ + 23); ESI^+/MS/MS *m/z* 292 (100); ^1H NMR (300 MHz): δ 1.80–1.92 (m, 4H), 2.18–2.28 (m, 1H), 2.45–2.62 (m, 4H), 2.95–3.05 (m overlapping s at 3.04, 2H), 3.04 (s overlapping m at 2.95–3.05, 3H), 3.10–3.18 (m, 1H), 3.81 (s, 3H), 3.88–3.98 (m, 2H), 4.02–4.12 (m, 1H), 6.58–6.66 (m, 1H), 6.76 (ddd, *J* = 11.8, 6.6, 3.0 Hz, 1H), 6.88 (dd, *J* = 8.8, 2.8 Hz, 1H), 7.06 (apparent q, 1H), 7.14 (d, *J* = 2.8 Hz, 1H), 7.44 (d, *J* = 8.8 Hz, 1H); ^{13}C NMR (75 MHz): 29.0 (1C), 29.4 (1C), 32.7 (1C), 51.9 (1C), 55.1 (1C), 57.8 (1C), 60.4 (2C), 65.9 (1C), 71.2 (1C), 104.5 (d, $^2J_{CF}$ = 20.2 Hz, 1C, ArO *C*-2), 105.4 (1C), 110.1 (m, 1C, ArO *C*-6), 113.7 (1C), 117.4 (d, $^2J_{CF}$ = 18.5 Hz, 1C, ArO *C*-5), 119.3 (1C), 131.4 (1C), 145.4 (dd, $^1J_{CF}$ = 239.0 Hz, $^2J_{CF}$ = 12.5 Hz, 1C, ArO *C*-4), 147.3 (1C), 150.6 (dd, $^1J_{CF}$ = 246.1 Hz, $^2J_{CF}$ = 14.2 Hz, 1C, ArO *C*-3), 154.9 (1C), 155.2 (m, 1C, ArO *C*-1), 167.5 (1C). (*RS*)-1-{4-[6-Methoxy-1,3-benzothiazol-2-yl(methyl)amino] piperidin-1-yl}-3-(3,4-difluorophenoxy)propan-2-ol hydrochloride [(*RS*)-**15g**·HCl]: Yield: 28%; mp 195–198 °C (EtOH/THF); Anal. Calcd for $C_{23}H_{27}F_2N_3O_3S{\cdot}1.5HCl{\cdot}0.5H_2O$: C, 52.39; H, 5.64; N, 7.97. Found: C, 52.08; H, 5.59; N, 7.68.

*4.1.1.14. (RS)-1-{4-[6-Trifluoromethyl-1,3-benzothiazol-2-yl(methyl) amino]piperidin-1-yl}-3-(3,4-difluorophenoxy)propan-2-ol [(RS)-**15h**].* The title compound was prepared starting from (*RS*)-**12a** and **14d**: Yield: 43%; IR (neat): 3372 (OH) cm^{-1}; ESI^+/MS: 524 (M^+ + 23); ESI^+/MS/MS *m/z* 292 (100); ^1H NMR (300 MHz, $CDCl_3$): δ 1.85–2.05 (m, 4H), 2.32 (dt, *J* = 11.3, 3.3 Hz, 1H), 2.45–2.72 (m, 4H), 3.09 (s overlapping m at 3.08–3.18, 3H), 3.08–3.18 (m overlapping s at 3.09, 1H), 3.20–3.28 (m, 1H), 3.94 (d, *J* = 5.0 Hz, 2H), 4.08–4.18 (m, 1H), 4.20–4.32 (m, 1H), 6.58–6.66 (m, 1H), 6.76 (ddd, *J* = 11.8, 6.3, 3.0 Hz, 1H), 7.06 (apparent q, 1H), 7.48–7.60 (m, 2H), 7.84 (s, 1H); ^{13}C NMR (75 MHz, $CDCl_3$): 28.7 (1C), 29.0 (1C), 33.1 (1C), 52.0 (1C), 55.0 (1C), 57.7 (1C), 60.5 (2C), 65.8 (1C), 71.2 (1C), 104.5 (d, $^2J_{CF}$ = 20.2 Hz, 1C, ArO *C*-2),11 0.1 (m, 1C, ArO *C*-6), 117.4 (d, $^2J_{CF}$ = 18.5 Hz, 1C, ArO *C*-5), 118.6 (1C), 122.9 (1C), 123.0 (1C), 126.6 (1C), 130.7 (1C), 145.4 (dd, $^1J_{CF}$ = 239.0 Hz, $^2J_{CF}$ = 12.5 Hz, 1C, ArO *C*-4), 150.7 (dd, $^1J_{CF}$ = 246.3 Hz, $^2J_{CF}$ = 14.0 Hz, 1C, ArO *C*-3), 155.1 (dd, $^2J_{CF}$ = 8.2 Hz, $^3J_{CF}$ = 2.2 Hz, 1C, ArO *C*-1), 155.6 (1C), 170.5 (1C). (*RS*)-1-{4-[6-Trifluoromethyl-1,3-benzothiazol-2-yl(methyl)amino]piperidin-1-yl}-3-(3,4-difluorophenoxy)propan-2-ol hydrochloride [(*RS*)-**15h**·HCl]: Yield: 17%; mp 201–203 °C (EtOH); Anal. Calcd for $C_{23}H_{24}F_5N_3O_2S{\cdot}2HCl{\cdot}H_2O$: C, 46.63; H, 4.76; N, 7.09. Found: C, 46.82; H, 4.53; N, 6.92.

*4.1.1.15. (RS)-1-{4-[6-Hydroxy-1,3-benzothiazol-2-yl(methyl)amino] piperidin-1-yl}-3-(3,4-difluorophenoxy)propan-2-ol [(RS)-**15i**].* The title compound was prepared starting from (*RS*)-**12a** and **14e**: Yield: 48%; IR (neat): 3402 (OH) cm^{-1}; ESI^+/MS: 450 (M^+ + H); ESI^+/MS/MS *m/z* 270 (100); ^1H NMR (300 MHz): δ 1.75–1.95 (m, 4H), 2.15–2.30 (m, 1H), 2.40–2.68 (m, 4H), 2.95–3.08 (m overlapping s at 3.00, 2H), 3.00 (s overlapping m at 2.95–3.08, 3H), 3.10–3.20 (m, 1H), 3.91 (d, *J* = 5.0 Hz, 2H), 4.02–4.15 (m, 2H), 6.55–6.65 (m, 1H), 6.74 (ddd, *J* = 12.1, 6.6, 3.0 Hz, 1H), 6.80 (dd, *J* = 8.5, 2.5 Hz, 1H), 7.04 (apparent q overlapping d at 7.10, 1H), 7.10 (d overlapping apparent q at 7.04, *J* = 2.8 Hz, 1H), 7.36 (d, *J* = 8.5 Hz, 1H). (*RS*)-1-{4-[6-Hydroxy-1,3-benzothiazol-2-yl (methyl)amino]piperidin-1-yl}-3-(3,4-difluorophenoxy)propan-2-ol phosphate [(*RS*)-**15i**·H_3PO_4]: Yield: 15 %; mp 160–162 °C (MeOH/Et_2O); ^{13}C NMR (75 MHz, CD_3OD): 25.4 (1C), 32.0 (2C), 47.8 (2C, overlapping CD_3OD), 51.7 (1C), 54.4 (1C), 64.2 (1C), 70.6 (1C), 103.9 (d, $^2J_{CF}$ = 20.6 Hz, 1C, ArO *C*-2), 106.3 (1C), 110.0 (m, 1C, ArO *C*-6), 114.2 (1C), 116.9 (d, $^2J_{CF}$ = 17.2 Hz, 1C, ArO *C*-5), 118.3 (1C), 130.5 (1C), 145.0 (dd, $^1J_{CF}$ = 237.4 Hz, $^2J_{CF}$ = 12.2 Hz, 1C, ArO *C*-4), 145.1 (1C), 150.2 (dd, $^1J_{CF}$ = 244.1 Hz, $^2J_{CF}$ = 13.4 Hz, 1C, ArO *C*-3), 155.1 (d, $^2J_{CF}$ = 10.8 Hz, 1C, ArO *C*-1), 152.3 (1C), 167.4 (1C). Anal. Calcd for $C_{22}H_{25}F_5N_3O_3S{\cdot}2H_3PO_4$: C, 40.93; H, 4.84; N, 6.51. Found: C, 40.69; H, 4.91; N, 6.26.

*4.1.1.16. (RS)-1-{4-[1,3-Benzothiazol-2-yl(methyl)amino]piperidin-1-yl}-3-(3-methoxyphenoxy)propan-2-ol [(RS)-**15l**].* The title compound

was prepared starting from (*RS*)-**12b** and commercially available 2-chlorobenzothiazole: Yield: 42%; IR (neat): 3402 (OH) cm^{-1}; ESI^+/MS: 450 ($M^+ + Na$); ESI^+/MS/MS *m/z* 286 (100); ^1H NMR (500 MHz): δ 1.84–2.02 (m, 4H), 2.28 (dt, $J = 11.5$, 3.0 Hz, 1H), 2.54 (dt, $J = 11.8$, 2.3 Hz, 1H), 2.59 (dd, $J = 12.7$, 3.9 Hz, 1H), 2.65 (dd, $J = 12.5$, 9.5 Hz, 1H), 3.05 (br d overlapping s at 3.08, $J = 9.8$ Hz, 1H), 3.08 (s overlapping br d at 3.05, 3H), 3.18 (br d, $J = 9.8$ Hz, 1H), 3.80 (s, 3H), 3.99 (d, $J = 4.9$ Hz, 2H), 4.08–4.15 (m, 2H), 4.16–4.22 (m, exch. D_2O, 1H), 6.50–6.56 (m, 3H), 7.06 (apparent t, 1H), 7.19 (apparent t, 1H), 7.25–7.32 (m, 1H), 7.58 (d, $J = 8.3$ Hz, 1H), 7.60 (d, $J = 7.8$ Hz, 1H); ^{13}C NMR (125 MHz): 28.7 (1C), 29.0 (1C), 32.6 (1C), 51.9 (1C), 54.8 (1C), 55.3 (1C), 60.4 (1C), 60.5 (1C), 65.8 (1C), 70.2 (1C), 101.1 (1C), 106.7 (2C), 118.7 (1C), 120.6 (1C), 121.0 (1C), 125.9 (1C), 129.9 (1C), 130.3 (1C), 152.9 (1C), 159.9 (1C), 160.8 (1C), 168.7 (1C). (*RS*)-1-{4-[1,3-Benzothiazol-2-yl(methyl)amino]piperidin-1-yl}-3-(3-methoxyphenoxy)propan-2-ol hydrochloride [(*RS*)-**15l**·HCl]: Yield: 18%; mp 195–196 °C (abs EtOH/THF); Anal. Calcd for $C_{23}H_{29}N_3O_3S{\cdot}2HCl{\cdot}H_2O$: C, 53.28; H, 6.42; N, 8.10. Found: C, 53.67; H, 6.15; N, 8.16.

*4.1.1.17. (RS)-1-{4-[6-Methoxy-1,3-benzothiazol-2-yl(methyl)amino] piperidin-1-yl}-3-(3-methoxyphenoxy)propan-2-ol [(RS)-**15m**].* The title compound was prepared starting from (*RS*)-**12b** and **14c**: Yield: 34%; IR (neat): 3324 (OH) cm^{-1}; ESI^+/MS: 458 ($M^+ + H^+$); ESI^+/MS/MS *m/z* 264 (100); ^1H NMR (500 MHz): δ 1.80–2.02 (m, 4H), 2.32 (t, $J = 11.0$ Hz, 1H), 2.57 (t, $J = 11.3$ Hz, 1H), 2.64 (dd, $J = 12.7$, 3.9 Hz, 1H), 2.69 (apparent t, 1H), 3.05 (s, 3H), 3.11 (br d, $J = 11.3$ Hz, 1H), 3.23 (br d, $J = 11.7$ Hz, 1H), 3.80 (s, 3H), 3.82 (s, 3H), 3.90–4.02 (m, 2H), 4.10–4.20 (m, 2H), 4.78 (br s, exch. D_2O, 1H), 6.51 (s, 1H), 6.53 (d, $J = 8.3$ Hz, 2H), 6.90 (dd, $J = 8.6$, 1.7 Hz, 1H), 7.15 (s, 1H), 7.19 (apparent t, 1H), 7.45 (d, $J = 8.8$ Hz, 1H); ^{13}C NMR (125 MHz): 28.4 (1C), 28.7 (1C), 32.5 (1C), 52.0 (1C), 54.9 (1C), 55.3 (1C), 55.9 (1C), 60.4 (1C), 60.6 (1C), 65.7 (1C), 70.1 (1C), 101.1 (1C), 105.2 (1C), 106.6 (1C), 106.7 (1C), 113.5 (1C), 119.1 (1C), 129.9 (1C), 131.2 (1C), 147.1 (1C), 154.7 (1C), 159.9 (1C), 160.8 (1C), 167.3 (1C). (*RS*)-1-{4-[6-Methoxy-1,3-benzothiazol-2-yl(methyl)amino]piperidin-1-yl}-3-(3-methoxyphenoxy) propan-2-ol hydrochloride [(*RS*)-**15m**·HCl]: Yield: 14%; mp 186–187 °C (abs EtOH/THF); Anal. Calcd for $C_{24}H_{31}N_3O_4S{\cdot}2HCl{\cdot}H_2O$: C, 52.55; H, 6.43; N, 7.66. Found: C, 52.84; H, 6.25; N, 7.52.

*4.1.1.18. General procedure for synthesizing compounds (RS)-**16n,o**.* The method adopted for the synthesis of (*RS*)-1-{4-[1,3-benzothiazol-2-yl (methyl)amino]piperidin-1-yl}-3-(3-hydroxyphenoxy)propan-2-ol [(*RS*)-**16n**] is described.

Aluminum chloride (0.180 g, 1.4 mmol) was added to a solution of (*RS*)-1-{4-[1,3-benzothiazol-2-yl(methyl)amino]piperidin-1-yl}-3-(3-methoxyphenoxy)propan-2-ol [(*RS*)-**15l**] (0.116 g, 0.3 mmol) in toluene (4.7 mL) and the mixture was heated at 110 °C for 18 h. The reaction mixture was cooled to room temperature and 1 M HCl (4.4 mL) was added. After evaporation of the organic solvent, the aqueous phase was washed with EtOAc, alkaline was made with NaOH pellets, and EtOAc was extracted. The combined organic phases were dried over anhydrous Na_2SO_4, and concentrated in vacuo to give 0.101 g of a pink solid (81%) which was recrystallized from EtOAc (43%): mp 191–193 °C (EtOAc); IR (neat): 3460 (OH) cm^{-1}; ESI^+/MS: 412 ($M^+ - H^+$); ESI^+/MS/MS *m/z* 163 (100); ^1H NMR (500 MHz, CD_3OD + Pyridine-d_5): δ 1.12–1.20 (m, 2H), 1.61 (br d, $J = 12.2$, Hz, 2H), 1.75–1.90 (m, 2H), 2.10–2.25 (m, 2H), 2.55–2.62 (m, 1H), 2.92 (s, 3H), 3.00–3.10 (m, 2H), 3.95–4.02 (m, 1H), 4.05 (dd, $J = 9.8$, 4.4 Hz, 1H), 4.15–4.22 (m, 1H), 6.51 (d, $J = 8.3$ Hz, 1H), 6.58 (d, $J = 8.8$ Hz, 1H), 6.65 (apparent t, 1H), 7.00 (apparent t, 1H), 7.10 (apparent t, 1H), 7.24 (apparent t, 1H), 7.54 (d, $J = 7.3$ Hz, 1H), 7.60 (d, $J = 7.8$ Hz, 1H). ^{13}C NMR (125 MHz, $CDCl_3$ + CD_3OD): 28.6 (1C), 28.8 (1C), 32.4 (1C), 52.3 (1C), 54.2 (1C), 60.6 (1C), 66.4 (1C), 70.2 (1C), 102.0 (1C), 105.7 (1C), 108.2 (1C), 118.2 (1C), 120.5 (1C), 121.1 (1C), 126.0 (1C), 129.6 (1C), 129.9 (1C), 152.2 (1C), 158.0 (1C), 159.9 (2C), 169.1 (1C). Anal. Calcd for $C_{22}H_{27}N_3O_3S.0.33H_2O$: C, 62.98; H, 6.65; N, 10.02. Found: C, 63.32; H, 6.55; N, 9.90.

*4.1.1.19. (RS)-1-{4-[6-Hydroxy-1,3-benzothiazol-2-yl(methyl)amino] piperidin-1-yl}-3-(3-hydroxyphenoxy)propan-2-ol [(RS)-**16o**].* The title compound was prepared starting from (*RS*)-**15m**: Yield: 88%; IR (neat): 3062 (OH) cm^{-1}; ESI^+/MS: 428 ($M^+ - H^+$); ESI^+/MS/MS *m/z* 318 (100). (*RS*)-1-{4-[6-Hydroxy-1,3-benzothiazol-2-yl(methyl)amino] piperidin-1-yl}-3-(3-hydroxyphenoxy)propan-2-ol phosphate [(*RS*)-**16o**·H_3PO_4]: Yield: 24%; mp 195–196 °C (abs EOH/THF); ^1H NMR (500 MHz, CD_3OD): δ 2.06 (br t, $J = 13.2$, Hz, 2H), 2.23–2.45 (m, 2H), 3.31 (s, 3H), 3.20–3.45 (m, 3H), 3.78–3.85 (m, 3H), 3.96 (dd, $J = 9.8$, 5.4 Hz, 1H), 4.02 (dd, $J = 9.8$, 4.9 Hz, 1H), 4.38–4.50 (m, 2H), 6.40–6.48 (m, 3H), 6.80 (dd, $J = 8.8$, 2.4 Hz, 1H), 7.07 (d, $J = 8.3$ Hz, 1H), 7.10 (d, $J = 2.4$ Hz, 1H), 7.33 (d, $J = 8.8$ Hz, 1H); ^{13}C NMR (125 MHz, CD_3OD): 25.4 (2C), 32.1 (1C), 51.7 (2C), 54.5 (2C), 64.3 (1C), 69.7 (1C), 101.7 (1C), 105.3 (1C), 106.4 (1C), 108.1 (1C), 114.2 (1C), 118.4 (1C), 129.6 (1C), 130.6 (1C), 145.0 (1C), 152.6 (1C), 158.4 (1C), 159.7 (1C), 167.3 (1C). Anal. Calcd for $C_{22}H_{27}N_3O_4S{\cdot}2H_3PO_4$: C, 42.24; H, 5.32; N, 6.72. Found: C, 42.22; H, 5.53; N, 6.68.

4.2. Pharmacology

4.2.1. hERG electrophysiological recordings

Patch-clamp studies were carried out on Human Embryonic Kidney (HEK) 293 cells stably transfected with hERG1a isoform (DI.V.A.L. Toscana srl, Italy). Electrophysiological recordings were performed using the whole-cell mode of the patch-clamp technique. The extracellular solution used for patch-clamp recordings had the following composition: 140 mM NaCl, 5 mM KCl, 1 mM $MgCl_2$, 2 mM $CaCl_2$, 10 mM Glucose, 10 mM HEPES, pH 7.4 with NaOH. The pipette contained: 145 mM KCl, 10 mM EGTA, 1 mM $MgCl_2$, 2 mM Mg-ATP, 10 mM HEPES, pH 7.30 with KOH. To elicit the activating outward current, a depolarizing step from a holding potential of −80 mV–0 mV (3 s in duration) was applied. A tail current was then evoked by repolarizing to −40 mV for 3 s. Successive command pulses were applied at 10-s intervals. IC_{50} values for lubeluzole analogues were determined based on the extent of hERG tail current inhibition, as previously described [4]. The mean values, after normalization, were plotted and fitted with the Hill equation, yielding the corresponding IC_{50} and Hill slope (n_H) values. Solutions were applied to the cell via a gravity-fed perfusion system (VC-6 Six Channel Valve Controller, Warner Instruments). Patch-clamp electrodes were pulled from Sutter capillary glass (Novato, CA) on a Flaming/Brown type puller (Sutter P-87), and fire polished to 3–4 MΩ resistance, using a microforge (Narishige). Patch-clamp recordings of cell cultures were carried out at room temperature 48h after transfection. For recordings a Multiclamp 200B amplifier (Molecular Devices, Inc, Sunnyvale, CA) and Digidata 1440 data acquisition board (Molecular Devices, Inc, Sunnydale, CA) with pCLAMP 10 software (Molecular Devices, Inc, Sunnyvale, CA) were used. Data analysis was performed using Origin 8.0 (OriginLab Corporation, Northampton, MA).

4.2.2. Voltage-gated sodium channel

4.2.2.1. In vitro experiments. The HEK293T cells were permanently or transiently transfected with hNav1.4 and hNav1.5, respectively, as previously described [17,46]. Whole-cell sodium currents were recorded using patch-clamp technique at room temperature (20 ± 2 °C) with Axopatch-1D amplifier, Digidata-1440A interface, and PClamp 10.6 software (Molecular Devices Ltd, UK). Glass pipettes were obtained using a vertical puller (Narishige, Japan) and filled in with intracellular solution containing (in mM) 120 CsF, 10 CsCl, 10 NaCl, 5 EGTA, and 5 HEPES (pH set to 7.2 with CsOH). External bath solution contained (in mM) 150 NaCl, 4 KCl, 2 CaCl2, 1 MgCl2, 5 HEPES, and 5 glucose (pH set to 7.4 with NaOH). With these solutions, the patch pipette resistance was in between 1.5 and 3.0 MΩ. Sodium currents were allowed to

stabilize for ~5 min in the whole-cell configuration before recording using the voltage-clamp protocols reported in the figures. The patched cells were constantly superfused with external solution, either control or supplemented with the desired compound concentration. Lubeluzole (**15f**) and **16o** were solubilized at 300 μM in bath patch solution using 0.2% dimethylsulfoxide (DMSO), and final concentrations were obtained by further dilution in bath solution. DMSO 0.2% has no effect on sodium currents. The concentration-response relationships were constructed with data obtained in different cells tested with a maximum of two drug concentrations and were fitted to a standard Hill equation (reported in figures).

4.2.2.2. In vivo experiments. Animal housing and experiments were performed in accordance with the Italian law for the use and care of laboratory animals (D.Lgs 26/2014), which conforms to the European Union Directive for the protection of experimental animals (2010/63/EU). The project 19 was approved by the Committee in charge of Animal Welfare of the University of Bari (OPBA n. 31829-X/10) and Italian Health Department (n. 647/2017-PR). All efforts were made to minimize animal suffering and to reduce the number of animals used. Six adult Wistar rats (body weight: 350/500 g; Charles River Laboratories, Calco, Italy) received water and food ad libitum. To induce myotonia, the rats received intraperitoneal injection of 30 mg/kg 9-anthracene carboxylic acid (9-AC) [9,30,47]. Through inhibition of the skeletal muscle chloride channels, 9-AC induces muscle stiffness resembling myotonia congenita, the genetic disease due to loss-of-function mutations in ClC-1 channel [48]. The 9-AC effects develop a few minutes after i.p. injection, reach maximum within 1 h, and then gradually decreased up to full recovery in 3–4 h [30]. The myotonia was quantified by the time of righting reflex (TRR), which is the time needed by the rat placed in supine position to turn back on its four limbs. In control conditions, the TRR is less than half a second, but it increases to 3–4 s at the maximal effect of 9-AC. An antimyotonic drug is expected to reduce the 9-AC-induced TRR. Each experiment was performed in 3 rats simultaneously, one receiving 1 mg/kg lubeluzole (**15f**), one receiving 1 mg/kg **16o**, and one receiving drug vehicle only (normal saline). The drugs were given orally 20 min after 9-AC injection using an esophageal cannula. The TRR was determined 10 min before 9-AC injection and 10, 30, 60, 120 and 180 min after 9-AC. At each time point, the TRR value was calculated as the mean of 7 determinations, repeated at 1-min intervals. In each animal, TRR values were then normalized with respect to TRR measured 10 min after 9-AC. The experiments was repeated 3 times, and values are reported as mean ± S.E.M. (standard error of the mean).

4.2.3. Radioligand binding studies

Binding affinities towards the adrenergic receptors α_{1A}-AR and β_2-AR were determined as described previously [49,50]. In brief, membranes were prepared from HEK293T cells transiently transfected with the cDNA for the human adrenoreceptors α_{1A}-AR and β_2-AR (both from cDNA Resource Center, Bloomsburg University, Bloomsberg, PA). For homogenates from α_{1A}-AR expressing cells a receptor density of B_{max} = 2,700 ± 100 fmol/mg and a specific binding affinity for the radioligand [^{3}H]prazosin (specific activity 78 Ci/mmol, Novandi, Södertälje, Sweden) was determined with a K_D value of 0.40 ± 0.050 nM. Membranes carrying the β_2-AR showed a B_{max} of 3,600 fmol/mg and a K_D = 0.095 nM with the radioligand [^{3}H]CGP12,177 (specific activity 38 Ci/mmol, Biotrend, Cologne, Germany). Competition binding experiments were performed by incubating membranes in binding buffer (for α_{1A}-AR: 50 mM Tris, 5 mM $MgCl_2$, 0.1 mM EDTA, 5 μg/mL bacitracin and 5 μg/mL soybean trypsin inhibitor at pH 7.4; for β_2-AR: 25 mM HEPES, 5 mM $MgCl_2$, 1 mM EDTA, and 0.006% bovine serum albumin at pH 7.4) at final protein concentration of 4 μg/well for α_{1A}-AR and 3 μg/well for β_2-AR together with the radioligand (0.4 nM of [^{3}H]prazosin, 0.2 nM of [^{3}H]CGP12,177) and varying concentrations of the competing ligands. After an incubation for 60 min at 37 °C membrane bound radioactivity was separated by filtration on GF/B glass fiber mats and counted in a scintillation counter (Microbeta from PerkinElmer, Rodgau, Germany). Non-specific binding was determined in the presence of non-labeled prazosine and CGP12,177 each at a final concentration of 10 μM. The protein concentration was determined applying the method of Lowry [51]. The resulting competition curves were analyzed by nonlinear regression using the algorithms implemented in PRISM 10.2 (GraphPad Software, San Diego, CA) to get IC_{50} values, which were subsequently transformed into the K_i values employing the equation of Cheng and Prusoff [52].

4.2.4. Ex vivo functional studies

Guinea pigs of either sex (200–400 g) from Charles River (Calco, Como, Italy) were used. The animals were housed according to the ECC Council Directive regarding the protection of animals used for experimental and other scientific purposes (Directive 2010/63/EU of the European Parliament and of the Council) and the WMA Statement on Animal Use in Biomedical Research. All procedures followed the guidelines of the animal care and use committee of the University of Bologna (Bologna, Italy). The ethical committee authorization was reported and numbered as "Protocol 2DBFE.N.YEV" by the Comitato Etico Scientifico for Animal Research Protocols according to D.L. vo 116/92 and approved by the Ministry of Health in December 2023.

Guinea-pigs were sacrificed by cervical dislocation. The ileum longitudinal smooth muscle was picked up and set up rapidly in warmed Tyrode solution bubbled with 95% O_2-5% CO_2, pH 7.4. used as described below. The procedure has already been previously described [53]. All data were analyzed using Student's test and are presented as mean ± S.E.M. Compounds were added in a cumulative manner and the potency, defined as IC_{50}, was evaluated from log concentration-response curves (Probit analysis using Litchfield and Wilcoxon) [37].

4.3. Molecular modelling methods

Compound **16o** was built in the *(S)* configuration starting from the lubeluzole X-ray data [54] relaxing thereafter the properly modified structure with the UFF and 10000 steps of Steepest Descent minimization as implemented in OpenBabel [55]. Oledaterol bound β_2-adrenoceptor structure (pdb code 8JJL) was recruited as target, and a quality check on this structure was acquired with the Protein Preparation Wizard interface of Maestro software package [56] removing water molecules, adding hydrogen atoms, optimizing their position, and assigning the ionization states of acid and basic residues according to PROPKA prediction at pH 7.0. Electrostatic charges for protein atoms were loaded according to AMBER UNITED force field [57], while the *molcharge* complement of QUACPAC [58] was used in order to achieve Marsili-Gasteiger charges for the inhibitors. Affinity maps were first calculated on a 0.375 Å spaced 90 × 90 × 90 Å^3 rectangular box, having the barycentre on the bounded agonist, and the transmembrane inner cavity space was sampled performing a conformational ligand search with 1000 runs of Lamarckian Genetic Algorithm (LGA). To do this task, AutoDock [59] using the GPU-OpenCL version [60] was selected as docking engine, enhancing scoring accuracy taking explicitly into account solvent effect and contribution by means of the hydration force field [61], and setting the number of energy evaluations and population size respectively to 10 M and 300.

Binding poses were screened applying **ESP**, an energy (**E**), similarity (**S**) and population (**P**) based rule where energy accounts for the AutoDock free energy of binding and the energy difference between the selected pose and the relative global minimum and the ligand efficacy, similarity is scored by the *Tanimoto_Combo* coefficient of ROCS [62] shape matching algorithm, **P** population encodes the cluster members figures, and the rule is valid once at least four out of five parameters are below certain thresholds in this instance equal to **FEB** ≤ −12.00, **ΔE** ≤ 2.00, **EFF** ≤ −0.450, **SIM** ≥ 0.400, **POP** ≥ 100.

CRediT authorship contribution statement

Maria Maddalena Cavalluzzi: Writing – review & editing, Writing – original draft, Supervision, Project administration, Investigation. **Roberta Gualdani:** Writing – review & editing, Investigation. **Alessandro Farinato:** Investigation. **Concetta Altamura:** Investigation. **Sabata Pierno:** Investigation. **Natalie Paola Rotondo:** Investigation. **Francesco Terlizzi:** Investigation. **Laura Beatrice Mattioli:** Investigation. **Maria Grazia Perrone:** Investigation. **Maria Cristina Lomuscio:** Software. **Giuseppe Felice Mangiatordi:** Software. **Nicola Antonio Colabufo:** Funding acquisition. **Antonio Carrieri:** Writing – review & editing, Software, Investigation. **Roberta Budriesi:** Writing – review & editing, Validation. **Peter Gmeiner:** Investigation. **Harald Huebner:** Investigation. **Jean-François Desaphy:** Writing – review & editing, Validation, Resources, Methodology, Formal analysis, Conceptualization. **Giovanni Lentini:** Writing – review & editing, Supervision, Resources, Project administration, Conceptualization.

Declaration of competing interest

The authors declare that they have no known competing financial interests or personal relationships that could have appeared to influence the work reported in this paper.

Acknowledgments

We thank Dr. Capodiferro for technical help.

Data availability

Data will be made available on request.

References

[1] J.V. Ly, J.A. Zavala, G.A. Donnan, Neuroprotection and thrombolysis: combination therapy in acute ischaemic stroke, Expet Opin. Pharmacother. 7 (2006) 1571–1581.
[2] C. Gandolfo, P. Sandercock, M. Conti, Lubeluzole for acute ischaemic stroke, Cochrane Database Syst. Rev. 1 (2002) CD001924.
[3] B. Le Grand, M. Dordain-Maffre, G.W. John, Lubeluzole-induced prolongation of cardiac action potential in rabbit Purkinje fibres, Fundam. Clin. Pharmacol. 14 (2000) 159–162.
[4] R. Gualdani, M.M. Cavalluzzi, F. Tadini-Buoninsegni, M. Convertino, P. Gailly, A. Stary-Weinzinger, G. Lentini, Molecular insights into hERG potassium channel blockade by lubeluzole, Cell. Physiol. Biochem. 45 (2018) 2233–2245.
[5] M.M. Cavalluzzi, M. Viale, C. Bruno, A. Carocci, A. Catalano, A. Carrieri, C. Franchini, G. Lentini, A convenient synthesis of lubeluzole and its enantiomer: evaluation as chemosensitizing agents on human ovarian adenocarcinoma and lung carcinoma cells, Bioorg. Med. Chem. Lett. 23 (2013) 4820–4823.
[6] M. Viale, G. Lentini, R. Gangemi, P. Castagnola, G. Milani, S. Ravera, N. Bertola, A. Carrieri, M.M. Cavalluzzi, Lubeluzole repositioning as chemosensitizing agent on multidrug-resistant human ovarian A2780/DX3 cancer cells, Molecules 27 (2022) 7870.
[7] M.M. Cavalluzzi, R. Budriesi, De Salvia, M. A, L. Quintieri, M. Piarulli, G. Milani, R. Gualdani, M. Micucci, I. Corazza, A. Rosato, M. Viale, L. Caputo, C. Franchini, G. Lentini, Lubeluzole: from anti-ischemic drug to preclinical antidiarrheal studies, Pharmacol. Rep. 73 (2021) 172–184.
[8] J.-F. Desaphy, R. Carbonara, T. Costanza, G. Lentini, M.M. Cavalluzzi, C. Bruno, C. Franchini, D.C. Camerino, Molecular dissection of lubeluzole use-dependent block of voltage-gated sodium channels discloses new therapeutic potentials, Mol. Pharmacol. 83 (2013) 406–415.
[9] J.-F. Desaphy, R. Carbonara, T. Costanza, D. Conte Camerino, Preclinical evaluation of marketed sodium channel blockers in a rat model of myotonia discloses promising antimyotonic drugs, Exp. Neurol. 255 (2014) 96–102.
[10] R. Gualdani, M.M. Cavalluzzi, G. Lentini, Recent trends in the discovery of small molecule blockers of sodium channels, Curr. Med. Chem. 23 (2016) 2289–2332.
[11] C. Bruno, A. Carocci, A. Catalano, M.M. Cavalluzzi, F. Corbo, C. Franchini, G. Lentini, V. Tortorella, Facile, alternative route to lubeluzole, its enantiomer, and the racemate, Chirality 18 (2006) 227–231.
[12] D.S. Shapenova, M.K. Belyatskii, L.P. Panicheva, Synthesis of aryloxyacetaldehydes and *N-(aryloxyethyl)cyclohexanamine hydrochloroides*, Russ. J. Org. Chem. 46 (2010) 1017–1020.
[13] M.M. Cavalluzzi, G. Lentini, A. Lovece, C. Bruno, A. Catalano, A. Carocci, C. Franchini, First synthesis and full characterization of mexiletine *N-carbonyloxy β-D-glucuronide*, Tetrahedron Lett. 51 (2010) 5265–5268.
[14] C. Bruno, M.M. Cavalluzzi, M.R. Rusciano, A. Lovece, A. Carriera, R. Pracella, G. Giannuzzi, L. Polimeno, M. Viale, M. Illario, C. Franchini, G. Lentini, The chemosensitizing agent lubeluzole binds calmodulin and inhibits Ca^{2+}/calmodulin-dependent kinase II, Eur. J. Med. Chem. 116 (2016) 36–45.
[15] C. Bruno, G. Lentini, A. Catalano, A. Carocci, A. Lovece, A. Di Mola, M. M. Cavalluzzi, P. Tortorella, F. Loiodice, G. Iaccarino, P. Campiglia, E. Novellino, C. Franchini, Microwave-assisted synthesis of KN-93, a potent and selective inhibitor of Ca^{2+}/calmoduline-dependent protein kinase II, Synthesis 24 (2010) 4193–4198.
[16] M. Roselli, A. Carocci, R. Budriesi, M. Micucci, M. Toma, L. Di Cesare Mannelli, A. Lovece, A. Catalano, M.M. Cavalluzzi, C. Bruno, A. De Palma, M. Contino, M. G. Perrone, N.A. Colabufo, A. Chiarini, C. Franchini, C. Ghelardini, S. Habtemariam, G. Lentini, Synthesis, antiarrhythmic activity, and toxicological evaluation of mexiletine analogues, Eur. J. Med. Chem. 121 (2016) 300–307.
[17] A. Farinato, M.M. Cavalluzzi, C. Altamura, C. Campanale, P. Laghetti, I. Saltarella, P. Delre, A. Barbault, N. Tarantino, G. Milani, N.P. Rotondo, Di Cesare Mannelli, L.; Ghelardini, C.; Pierno, S.; Mangiatordi, G. F.; Lentini, G.; Desaphy, J.-F. Development of riluzole analogs with improved use-dependent inhibition of skeletal muscle sodium channels, ACS Med. Chem. Lett. 14 (2023) 999–1008.
[18] Schrödinger release 2022-4: Qikprop, Schrödinger, LLC, New York, NY, USA, 2021.
[19] M.M. Cavalluzzi, P. Imbrici, R. Gualdani, A. Stefanachi, G.F. Mangiatordi, G. Lentini, O. Nicolotti, Human ether-à-go-go-related potassium channel: exploring SAR to improve drug design, Drug Discov. Today 25 (2020) 344–366.
[20] T.M. Creanza, P. Delre, N. Ancona, G. Lentini, M. Saviano, G.F. Mangiatordi, Structure-based prediction of hERG-related cardiotoxicity: a benchmark study, J. Chem. Inf. Model. 61 (2021) 4758–4770.
[21] P. Delre, G.J. Lavado, G. Lamanna, M. Saviano, A. Roncaglioni, E. Benfenati, G. F. Mangiatordi, D. Gadaleta, Ligand-based prediction of hERG-mediated cardiotoxicity based on the integration of different machine learning techniques, Front. Pharmacol. 13 (2022) 951083.
[22] F. Olleik, M.H. Kamareddine, J. Spears, G. Tse, T. Liu, G.X. Yan, Mexiletine: antiarrhythmic mechanisms, emerging clinical applications and mortality, Pacing Clin. Electrophysiol. 46 (2023) 1348–1356.
[23] C. Altamura, I. Saltarella, C. Campanale, P. Laghetti, J.-F. Desaphy, Drug repurposing in skeletal muscle ion channelopathies, Curr. Opin. Pharmacol. 68 (2023) 102329.
[24] M. De Bellis, A. De Luca, F. Rana, M.M. Cavalluzzi, A. Catalano, G. Lentini, C. Franchini, V. Tortorella, D. Conte Camerino, Evaluation of the pharmacological activity of the major mexiletine metabolites on skeletal muscle sodium currents, Br. J. Pharmacol. 149 (2006) 300–310.
[25] J.-F. Desaphy, A. Dipalma, T. Costanza, R. Carbonara, M.M. Dinardo, A. Catalano, A. Carocci, G. Lentini, C. Franchini, D. Conte Camerino, Molecular insights into the local anesthetic receptor within voltage-gated sodium channels using hydroxylated analogs of mexiletine, Front. Pharmacol. 3 (2012) 17.
[26] R. Gualdani, F. Tadini-Buoninsegni, M. Roselli, I. Defrenza, M. Contino, N. A. Colabufo, G. Lentini, Inhibition of hERG potassium channel by the antiarrhythmic agent mexiletine and its metabolite *m*-hydroxymexiletine, Pharmacol. Res. Perspect. 3 (2015) e00160.
[27] B. Le Grand, J.M. Talmant, J.P. Rieu, J.F. Patoiseau, G.W. John, Study of the interaction of lubeluzole with cardiac sodium channels, J. Cardiovasc. Pharmacol. 42 (2003) 581–587.
[28] G. Li, L. Zhang, The role of mexiletine in the management of long QT syndrome, J. Electrocardiol. 51 (2018) 1061–1065.
[29] J.-F. Desaphy, T. Costanza, R. Carbonara, D. Conte Camerino, In vivo evaluation of antimyotonic efficacy of β-adrenergic drugs in a rat model of myotonia, Neuropharmacology 65 (2013) 21–27.
[30] J.-F. Desaphy, R. Carbonara, T. Costanza, D. Conte Camerino, Preclinical evaluation of marketed sodium channel blockers in a rat model of myotonia discloses promising antimyotonic drugs, Exp. Neurol. 255 (2014) 96–102.
[31] G. Milani, M.M. Cavalluzzi, C. Altamura, A. Santoro, M. G Perrone, M. Muraglia, N. A. Colabufo, F. Corbo, E. Casalino, C. Franchini, I. Pisano, J.-F. Desaphy, A. Carrieri, A. Carocci, G. Lentini, Bioisosteric modification of To042: synthesis and evaluation of promising use-dependent inhibitors of voltage-gated sodium channels, ChemMedChem 16 (2021) 3588–3599.
[32] S.P. Cairns, F. Borrani, β-Adrenergic modulation of skeletal muscle contraction: key role of excitation-contraction coupling, J. Physiol 593 (2015) 4713–4727.
[33] H. Zouhal, C. Jacob, P. Delamarche, A. Gratas-Delamarche, Catecholamines and the effects of exercise, training and gender, Sports Med. 38 (2008) 401–423.
[34] F. Curci, F. Corbo, M.L. Clodoveo, L. Salvagno, A. Rosato, I. Corazza, R. Budriesi, M. Micucci, L.B. Mattioli, Polyphenols from olive-mill wastewater and biological activity: focus on irritable bowel syndrome, Nutrients 14 (2022) 1264.
[35] L.B. Mattioli, R. Budriesi, L. Camarda, E. Nardi, P.L. Rossi, L. Bondioli, I. Corazza, Biomechanical characterization of spontaneous and induced motility in small animals' gastrointestinal tissue for human nutraceutical and pharmaceutical purposes, J. Mech. Med. Biol. (2025), https://doi.org/10.1142/S0219519425400512.
[36] E. Carosati, P. Ioan, G.B. Barrano, S. Caccamese, B. Cosimelli, F.J. Devlin, E. Severi, D. Spinelli, S. Superchi, R. Budriesi, Synthesis and L-type calcium channel blocking activity of new chiral oxadiazolothiazinones, Eur. J. Med. Chem. 92 (2015) 481–489.
[37] R.J. Tallarida, R.B. Murray, Manual of Pharmacologic Calculations with Computer Programs, second ed., Springer-Verlag, New York, 1987.
[38] A.J. Kooistra, C. Munk, A.S. Hauser, D.E. Gloriam, An online GPCR structure analysis platform, Nat. Struct. Mol. Biol. 28 (2021) 875–878.
[39] R.W. Marquis, A.M. Lago, J.F. Callahan, R.E.L. Trout, M. Gowen, E.G. DelMar, B. C. Van Wagenen, S. Logan, S. Shimizu, J. Fox, E.F. Nemeth, Z. Yang, T. Roethke, B.

R. Smith, K.W. Ward, J. Lee, R.M. Keenan, P. Bhatnagar, Antagonists of the calcium receptor I. Amino alcohol-based parathyroid hormone secretagogues, J. Med. Chem. 52 (2009) 3982–3993.
[40] M. Nayak, Y. Jung, I. Kim, Syntheses of pterocarpenes and coumestans via regioselective cyclodehydration, Org. Biomol. Chem. 14 (2016) 8074–8087.
[41] D.N. Kommi, D. Kumar, K. Seth, A.K. Chakraborti, Protecting group-free concise synthesis of *(RS)/(S)-lubeluzole*, Org. Lett. 15 (2013) 1158–1161.
[42] Z. Zhou, K. Kasten, T. Kang, D.B. Cordes, A.D. Smith, Enantioselective synthesis in continuous flow: polymer-supported isothiourea-catalyzed enantioselective michael addition–cyclization with α-azol-2-ylacetophenones, Org. Process Res. Dev. 28 (2024) 2041–2049.
[43] L. Zhu, M. Zhang, M. Dai, A convenient synthesis of 2-mercapto and 2-chlorobenzothiazoles, J. Heterocycl. Chem. 42 (2005) 727–730.
[44] Z. Lu, L. Wang, M. Hughes, S. Smith, Q. Shen, *$nBu_4N^+[AgI(CF_3)_2]^-$: trifluoromethylated argentate derived from fluoroform and its reaction with (hetero)aryl diazonium salts*, Org. Lett. 26 (2024) 2773–2777.
[45] X. Zhang, W. Jiang, J.M. Richter, J.A. Bates, S.K. Reznik, S. Stachura, R. Rampulla, D. Doddalingappa, S. Ulaganathan, J. Hua, J.S. Bostwick, C. Sum, S. Posy, S. Malmstrom, J. Dickey, D. Harden, R.M. Lawrence, V.R. Guarino, W. A. Schumacher, P. Wong, J. Yang, D.A. Gordon, R.R. Wexler, E.S. Priestley, Discovery of potent and selective quinoxaline-based protease-activated receptor 4 (PAR4) antagonists for the prevention of arterial thrombosis, J. Med. Chem. 67 (2024) 3571–3589.
[46] A. Carocci, M. Roselli, R. Budriesi, M. Micucci, J.-F. Desaphy, C. Altamura, M. M. Cavalluzzi, M. Toma, G.I. Passeri, G. Milani, A. Lovece, A. Catalano, C. Bruno, A. De Palma, F. Corbo, C. Franchini, S. Habtemariam, G. Lentini, Synthesis and evaluation of voltage-gated sodium channel blocking pyrroline derivatives endowed with both antiarrhythmic and antioxidant activities, ChemMedChem 16 (2021) 578–588.
[47] M. De Bellis, R. Carbonara, J. Roussel, A. Farinato, A. Massari, S. Pierno, M. Muraglia, F. Corbo, C. Franchini, M.R. Carratù, A. De Luca, D. Conte Camerino, J.-F. Desaphy, Increased sodium channel use-dependent inhibition by a new potent analogue of tocainide greatly enhances in vivo antimyotonic activity, Neuropharmacology 113 (2017) 206–216.
[48] C. Altamura, J.-F. Desaphy, D. Conte, A. De Luca, P. Imbrici, Skeletal muscle ClC-1 chloride channels in health and diseases, Pflügers Archiv 472 (2020) 961–975.
[49] X. Xu, J. Shonberg, J. Kaindl, M.J. Clark, A. Stößel, L. Maul, D. Mayer, H. Hübner, K. Hirata, A.J. Venkatakrishnan, R.O. Dror, B.K. Kobilka, R.K. Sunahara, X. Liu, P. Gmeiner, Constrained catecholamines gain β2AR selectivity through allosteric effects on pocket dynamics, Nat. Commun. 14 (2023) 2138.
[50] H. Hübner, C. Haubmann, W. Utz, P. Gmeiner, Conjugated enynes as nonaromatic catechol bioisosteres: synthesis, binding experiments, and computational studies of novel dopamine receptor agonists recognizing preferentially the D3 subtype, J. Med. Chem. 43 (2000) 756–762.
[51] O.H. Lowry, N.J. Rosebrough, A.L. Farr, R.J. Randall, Protein measurement with the Folin phenol reagent, J. Biol. Chem. 193 (1951) 265–275.
[52] Y. Cheng, W.H. Prusoff, Relationship between the inhibition constant (K1) and the concentration of inhibitor which causes 50 percent inhibition (I_{50}) of an enzymatic reaction, Biochem. Pharmacol. 22 (1973) 3099–3108.
[53] G. Milani, R. Budriesi, E. Tavazzani, M.M. Cavalluzzi, L.B. Mattioli, D.V. Miniero, P. Delre, B.D. Belviso, M. Denegri, C. Cuocci, N.P. Rotondo, A. De Palma, R. Gualdani, R. Caliandro, G.F. Mangiatordi, A. Kumawat, C. Camilloni, S. Priori, G. Lentini, hERG stereoselective modulation by mexiletine-derived ureas: molecular docking study, synthesis, and biological evaluation, Arch. Pharm. 356 (2023) 2300116.
[54] O.M. Peeters, N.M. Blaton, De Ranter C. J. *(+)-(S)-1-{4-[(2-Benzothiazolyl)(methyl) amino]piperidyl}-3-(3,4-difluorophenoxy)-2-propanol (Lubeluzole)*, Acta Crystallogr. C51 (1995) 2129–2132.
[55] N.M. O'Boyle, M. Banck, C.A. James, C. Morley, T. Vandermeersch, G. R. Hutchison, Open babel: an open chemical toolbox, J. Cheminf. 3 (2011) 33.
[56] Schrödinger release 2024-4: bioluminate, Schrödinger, LLC, New York, NY, 2024.
[57] W.D. Cornell, P. Ciepak, C.I. Bayty, I.R. Gould, K.M. Merz, D.M. Ferguson, D. C. Spellmeyer, T. Fox, J.W. Caldwell, P.A. Kollman, A second generation force field for the simulation of proteins, nucleic acid, and organic molecules, J. Am. Chem. Soc. 117 (1995) 5179–5197.
[58] QUACPAC 1.7.0.2: OpenEye Scientific Software, Santa Fe, NM.
[59] G.M. Morris, D.S. Goodsell, R.S. Halliday, R. Huey, W.E. Hart, R.K. Belew, A. J. Olson, Automated docking using a Lamarckian genetic algorithm and an empirical binding free energy function, J. Comput. Chem. 19 (1998) 1639–1662.
[60] L. El Khoury, D. Santos-Martins, S. Sasmal, J. Eberhardt, G. Bianco, F.A. Ambrosio, L. Solis-Vasquez, A. Koch, S. Forli, D.L. Mobley, Comparison of affinity ranking using AutoDock-GPU and MM-GBSA scores for BACE-1 inhibitors in the D3R grand challenge 4, J. Comput. Aided Mol. Des. 33 (2019) 1011–1020.
[61] S. Forli, A.J. Olson, A force field with discrete displaceable waters and desolvation entropy for hydrated ligand docking, J. Med. Chem. 55 (2012) 623–638.
[62] OpenEye Scientific Software, ROCS, 3.4.0.4, OpenEye Scientific Software, Santa Fe, NM.